

Article

Design, Synthesis, and Anti-Inflammatory Activities of 12-Dehydropyxinol Derivatives

Yunxiao Wang^{1,†}, Xiaoliang Mi^{1,†}, Yuan Du^{1,†}, Shuang Li¹, Liping Yu¹, Meng Gao¹, Xiaoyue Yang¹, Zhihua Song¹, Hui Yu^{2,*} and Gangqiang Yang^{1,*}

¹ School of Pharmacy, Collaborative Innovation Center of Advanced Drug Delivery System and Biotech Drugs in Universities of Shandong, Key Laboratory of Molecular Pharmacology and Drug Evaluation (Yantai University), Ministry of Education, Yantai University, Yantai 264005, China

² College of Food Engineering, Ludong University, Yantai 264025, China

* Correspondence: zoehuihui@hotmail.com (H.Y.); oceanygq@ytu.edu.cn (G.Y.)

† These authors contributed equally to this work.

Abstract: Pyxinol skeleton is a promising framework of anti-inflammatory agents formed in the human liver from 20S-protopanaxadiol, the main active aglycone of ginsenosides. In the present study, a new series of amino acid-containing derivatives were produced from 12-dehydropyxinol, a pyxinol oxidation metabolite, and its anti-inflammatory activity was assessed using an NO inhibition assay. Interestingly, the dehydrogenation at C-12 of pyxinol derivatives improved their potency greatly. Furthermore, half of the derivatives exhibited better NO inhibitory activity than hydrocortisone sodium succinate, a glucocorticoid drug. The structure–activity relationship analysis indicated that the kinds of amino acid residues and their hydrophilicity influenced the activity to a great extent, as did *R/S* stereochemistry at C-24. Of the various derivatives, **5c** with an *N*-Boc-protected phenylalanine residue showed the highest NO inhibitory activity and relatively low cytotoxicity. Moreover, derivative **5c** could dose-dependently suppress iNOS, IL-1 β , and TNF- α via the MAPK and NF- κ B pathways, but not the GR pathway. Overall, pyxinol derivatives hold potential for application as anti-inflammatory agents.

Keywords: pyxinol; anti-inflammatory activity; ginsenosides; structure–activity relationship



Citation: Wang, Y.; Mi, X.; Du, Y.; Li, S.; Yu, L.; Gao, M.; Yang, X.; Song, Z.; Yu, H.; Yang, G. Design, Synthesis, and Anti-Inflammatory Activities of 12-Dehydropyxinol Derivatives. *Molecules* **2023**, *28*, 1307. <https://doi.org/10.3390/molecules28031307>

Academic Editor: Giuseppe Manfroni

Received: 30 December 2022

Revised: 26 January 2023

Accepted: 28 January 2023

Published: 30 January 2023



Copyright: © 2023 by the authors. Licensee MDPI, Basel, Switzerland. This article is an open access article distributed under the terms and conditions of the Creative Commons Attribution (CC BY) license (<https://creativecommons.org/licenses/by/4.0/>).

1. Introduction

Inflammation is the physiological defense response against infection and injury. Excessive and prolonged inflammation can cause damage and result in various chronic diseases, including respiratory diseases, neurodegenerative diseases, and cancer [1,2]. Glucocorticoids (GCs) are the most effective drugs that inhibit inflammation in clinical settings; however, their side effects are extremely serious [3]. Nonetheless, owing to a lack of other effective drugs, GCs continue to be widely used to treat diseases such as COVID-19 [4]. Therefore, there is an urgent need to develop safer and more effective anti-inflammatory agents.

Ginsenosides are the primary pharmacological ingredients of ginseng, the well-known orally administered herb that strengthens vitality, extends life, and supports a healthy heart [5]. To date, ginsenosides are known to possess antitumor, memory preserving, anti-inflammatory, and cardioprotective activities [5–8]. Especially, the anti-inflammatory effects are remarkable because their aglycones exhibit structural similarity with GCs [9,10]. 20S-Protopanaxadiol (PPD, Figure 1) is one such aglycone and has been reported to be the main intestinal metabolite of protopanaxadiol-type ginsenosides that exhibit superior anti-inflammatory activities [9,11]. Recently, pyxinol (Figure 1) has been identified as the main PPD metabolite in the human liver and has attracted special attention in drug development [12–14]. Pyxinol and its derivatives have been demonstrated to exert cardioprotective,

antibiotic, and multidrug resistance-reversal effects [15–25]. Furthermore, our recent investigations have described their anti-inflammatory effects. Structure–activity relationship analysis revealed that the effects of pyxinol derivatives are closely related to *R/S* stereochemistry at C-24, and that the C-3 is a modifiable position for drug development [26,27]. Subsequently, derivative Y13 was identified to display better anti-inflammatory activities than hydrocortisone sodium succinate (HSS), the clinically approved steroid drug belonging to GCs [26]. Y13 could suppress proinflammatory cytokines to reduce inflammation via nuclear factor κ B (NF- κ B) and MAPK pathways, which is consistent with 20S-PPD and parental ginsenosides [11,28].

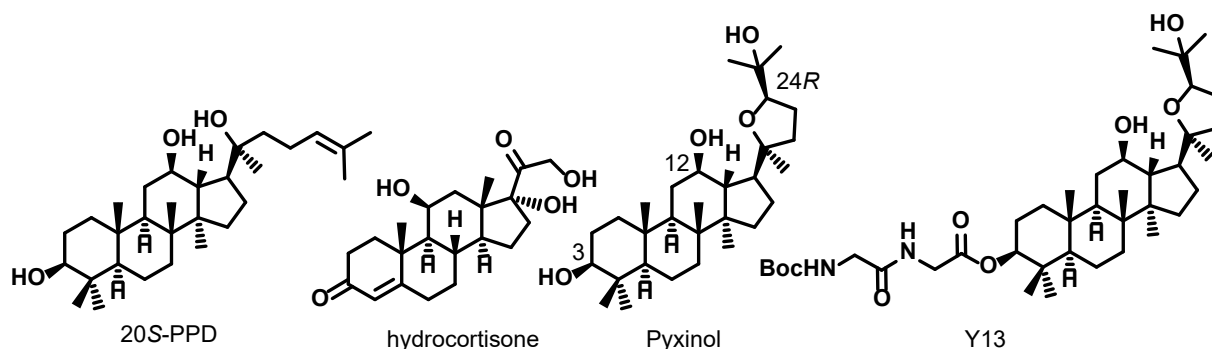


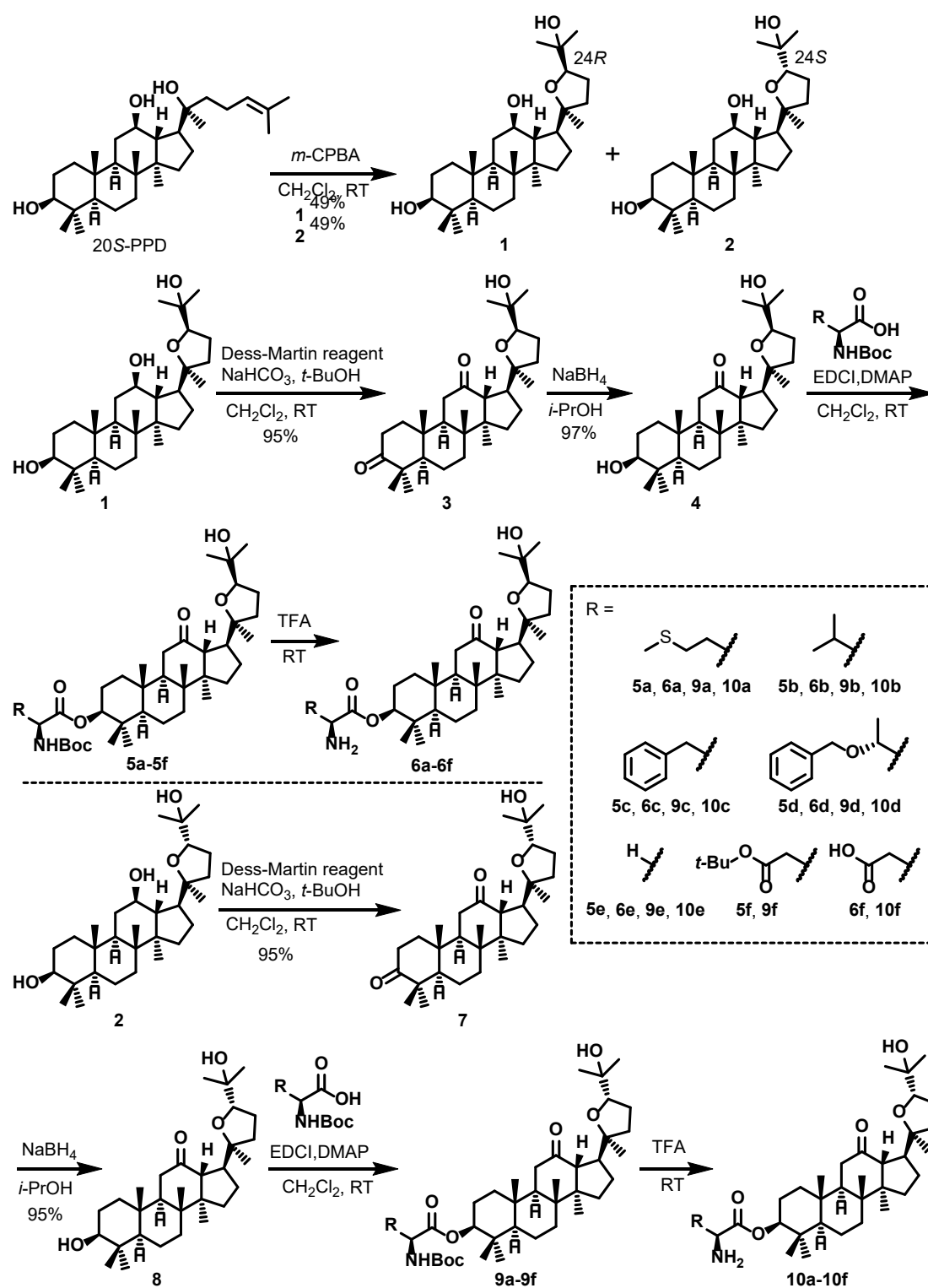
Figure 1. Chemical structures of 20S-PPD, hydrocortisone, pyxinol, and Y13.

Previous studies have reported that the 24*R*-epimer of pyxinol is selectively metabolized by CYP3A4 in the human liver to produce oxidation metabolites [14], such as 3-dehydropyxinol or 12-dehydropyxinol [12]. As the modification at C-3 could substantially improve the anti-inflammatory activities of pyxinol derivatives and the structural diversity of amino acids, 24 new 3-amino acid-12-dehydropyxinol derivatives were prepared in this study, and their anti-inflammatory effects in lipopolysaccharide (LPS)-induced macrophages were assessed. Of these, an *N*-Boc-protected phenylalanine derivative of 12-dehydropyxinol (5c) was identified to be the most potent compound and was used for mechanistic studies.

2. Results and Discussion

2.1. Chemistry

As described previously [16,29], pyxinol (1) and 24*S*-pyxinol (2) were obtained via the one step epoxidation of commercial 20*S*-PPD, which is shown in Scheme 1. 3,12-Didehydropyxinol was then synthesized via Dess–Martin oxidation and was subsequently selectively reduced in NaBH₄/isopropanol solution to obtain 12-dehydropyxinol with a yield of >90%. Amino acid-modified 12-dehydropyxinol derivatives (5a–5f) were next produced via DMAP-mediated esterification. Later, trifluoroacetic acid was utilized for *N*-Boc deprotection to obtain derivatives 6a–6f. The 24*S*-epimers (9a–9f, 10a–10f) were similarly synthesized from 24*S*-pyxinol.



Scheme 1. Synthesis of 12-dehydropyxinol derivatives.

2.2. NO-Inhibition of 12-Dehydropyxinol Derivatives

The inhibitory effect of specific compounds on LPS-triggered NO production is closely related to their anti-inflammatory activity [30,31]. Herein, the NO inhibition effects of all synthesized 12-dehydropyxinol derivatives were assessed in RAW264.7 macrophages using a Griess assay with HSS as the positive control. The cytotoxicity assay showed that most of the 12-dehydropyxinol derivatives did not display any evident toxic effects

on RAW264.7 cells, except **5f**, **6a**, **6f**, and **10d** when used at a concentration of 20 μM (Figure 2A). Then, these derivatives with no evident cytotoxicity were used for the NO inhibition assay. The treatment of RAW264.7 cells with 12-dehydropyxinol derivatives significantly suppressed the LPS-triggered NO production. Furthermore, most of the derivatives exhibited better NO inhibition activity than the parental compounds (**1**, **4**, **7**, and **8**) (Figure 2B), which agrees with previous results that modification at C-3 immensely improves anti-inflammatory activities [26,27]. Interestingly, most of the 12-dehydropyxinol derivatives also exhibited better NO inhibition activity than HSS, the positive control. Several of the 12-dehydropyxinol derivatives (**5a**, **5b**, **5c**, **5d**, **6e**, **10b**, and **10c**) exhibited even better NO inhibition activity than Y13, which has the highest potency among the known pyxinol derivatives with a hydroxy group at C-12. This observation suggests that dehydrogenation at C-12 of pyxinol can largely improve anti-inflammatory activity. Derivatives (**5a–5f** and **6e**) with a 24*R* configuration exhibited better potency than the corresponding 24*S* derivatives (**9a–9f** and **10e**), which is consistent with our previous findings that *R/S* stereochemistry at C-24 affects anti-inflammatory activity, with the 24*R*-configuration being preferred [26,27]. The modification types of amino acid residues at C-3 also largely affect their potency, with *N*-Boc-protected aromatic amino acids being preferred. This finding was quite different from pyxinol derivatives, in which *N*-Boc-protected neutral aliphatic amino acids were preferred, which suggests that the dehydrogenation at C-12 greatly influences the effect of the C-3 modification pattern on the improvement of anti-inflammatory activities. In most cases, the deprotection of Boc-protected amines reduced their anti-inflammatory effects, but not for the derivatives with an aromatic group. Based on the NO-inhibition activities of 12-dehydropyxinol derivatives, the structure–activity relationship (SAR) is summarized in Figure 3. Derivative **5c** with *N*-Boc-protected phenylalanine was identified to possess the highest NO inhibition activity and was selected for further studies.

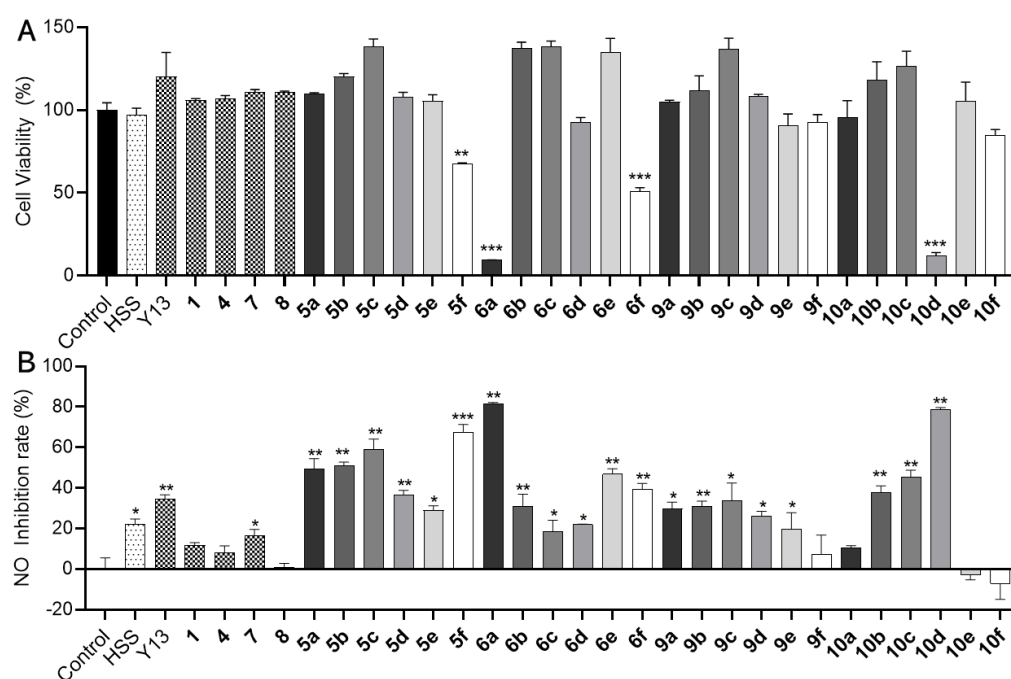


Figure 2. Inhibitory effects of 12-dehydropyxinol derivatives on LPS-triggered NO production in RAW264.7 macrophages: (A) Effect of 12-dehydropyxinol derivatives on cell survival and (B) LPS-triggered NO production. After pretreatment with test compounds (20 μM) for 2 h, the macrophages were treated with LPS (1 $\mu\text{g}/\text{mL}$) and further incubated for 24 h. Cell viability and nitrite concentrations were determined using MTT assays and Griess reaction, respectively. Data are expressed as the means \pm SD ($n = 3$): * $p < 0.05$, ** $p < 0.01$, *** $p < 0.001$ vs. control. HSS: hydrocortisone sodium succinate.

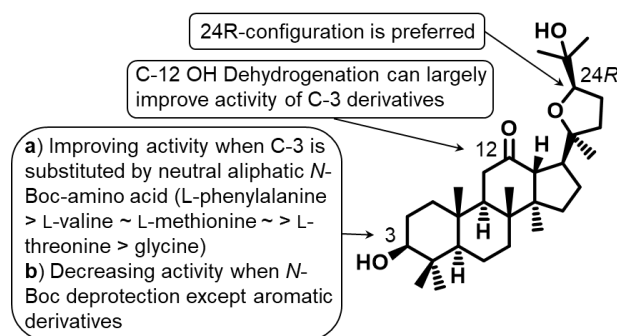


Figure 3. Preliminary structure–activity relationships of 12-dehydropyxinol derivatives.

2.3. Inhibition of LPS-Mediated Cytokines Production Using 5c

To fully confirm the anti-inflammatory effects of **5c**, the concentration dependent NO-inhibition assay was first assessed. As expected, the derivative **5c** could exert a NO-inhibitory effect in a concentration-dependent manner and even exhibit a significant NO-inhibitory effect as low as 1 μM , while the derivative **5c** exhibited no evident cytotoxicity at as high as 80 μM concentration (Figure 4A,B). Interleukin-1 β (IL-1 β) and tumor necrosis factor- α (TNF- α) are the other known proinflammatory cytokines that are rapidly yielded in inflammation and accelerated inflammatory progression [32]. We thus next evaluated its ability to inhibit IL-1 β and TNF- α production in RAW264.7 cells. LPS-triggered cells were treated with **5c** (5, 10, and 20 μM), after which the IL-1 β and TNF- α levels were measured using an enzyme-linked immunosorbent assay (ELISA), which indicated a marked upregulation in the levels of IL-1 β and TNF- α after LPS-induction, whereas the derivative **5c** concentration dependently suppressed this upregulation, which was even better than that of HSS (Figure 4C,D). These data further confirm the robust anti-inflammatory activities of derivative **5c**.

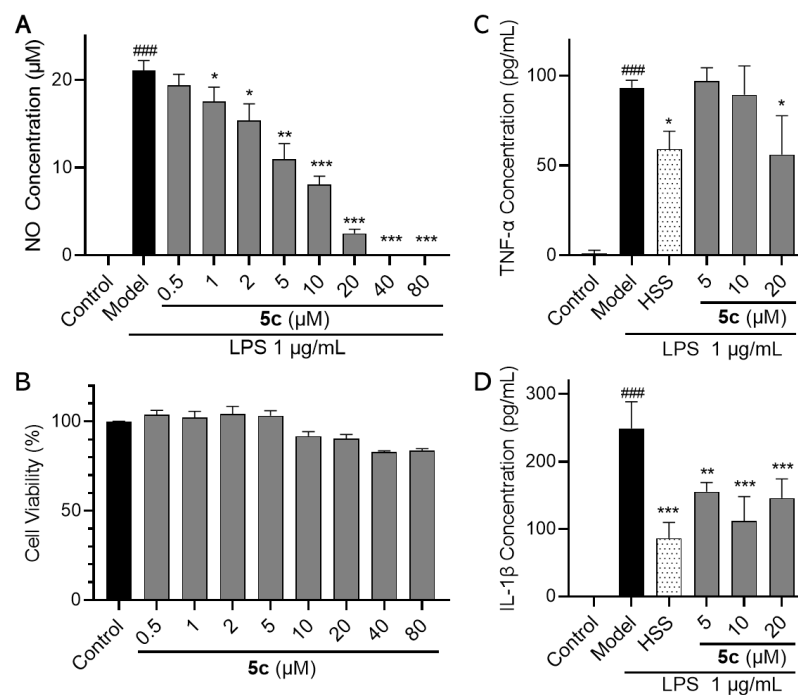


Figure 4. Anti-inflammatory effects of derivative **5c** on LPS-triggered RAW264.7 macrophages. The effects of derivative **5c** on (A) NO release, (B) the cytotoxicity, (C) TNF- α , and (D) IL-1 β secretion. The cells were evaluated following a (A,D) 24 h or (C) 6-h treatment with **5c** and LPS and (B) after 72-h treatment with **5c**. Data are expressed as the means \pm SD ($n = 3$): ### $p < 0.001$ vs. control; * $p < 0.05$, ** $p < 0.01$, *** $p < 0.001$ vs. model.

2.4. Inhibition of LPS-Mediated iNOS Upregulation and NF- κ B and MAPK Activation Using 5c

Inducible nitric oxide synthase (iNOS) is the key regulator of NO synthesis in response to inflammatory stimuli and aggravates inflammatory diseases [30,33]. We thus assessed the ability of 5c to regulate LPS-triggered iNOS expression via the 24-h treatment of RAW264.7 cells with 5c (5, 10, and 20 μ M) and LPS (1 μ g/mL). The resulting iNOS level was analyzed using Western blotting. In line with the promotion of NO production, LPS induced a significant upregulation of iNOS, whereas 5c suppressed this upregulation in a concentration-dependent manner (Figure 5). iNOS, IL-1 β , and TNF- α are positively regulated in inflammation by the NF- κ B pathway [34]. Both I κ B and NF- κ B p65 phosphorylation are key steps in the activated NF- κ B pathway, which lead to the upregulation of the above inflammation-related proteins. Subsequently, the impacts of 5c on LPS-triggered NF- κ B activation were assessed. Compound 5c inhibited LPS-triggered I κ B and NF- κ B p65 phosphorylation in a concentration-dependent manner, and these inhibitory effects of 5c were better than that of HSS (Figure 6A). PPD and other ginsenosides have been confirmed to exert anti-inflammatory effects by inhibiting the NF- κ B pathway, albeit weakly [9,28]. Our previous study has indicated that pyxinol might be the predominant active form of these ginsenosides that is responsible for the anti-inflammatory activity via the NF- κ B pathway [27]. 24R-epimer of pyxinol is preferentially metabolized in the human liver via oxidation, with dehydrogenation being one of the main forms of oxidation [12,13]. Together, these results, therefore, suggest that 12-dehydropyxinol derivatives may be the active forms of ginsenosides in humans, which exert anti-inflammatory effects and prevent the upregulation of inflammatory proteins by inhibiting NF- κ B activation.

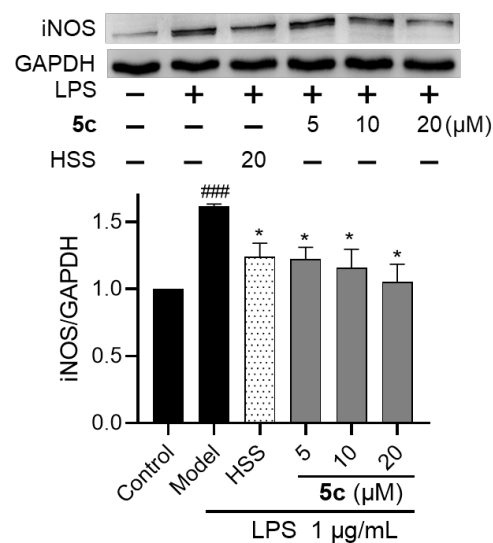


Figure 5. The impact of derivative 5c on LPS-triggered iNOS protein expression in RAW264.7 macrophages following 24-h treatment with a combination of LPS (1 μ g/mL) and 5c or HSS. Data are expressed as means \pm SD ($n = 3$) from triplicate experiments. ### $p < 0.001$ vs. control; * $p < 0.05$ vs. model.

The MAPK pathway is another major pathway that is activated to upregulate inflammatory proteins, such as iNOS and IL-1 β , in inflammatory stimuli [35]. c-Jun N-terminal kinase (JNK), extracellular regulated protein kinases (ERK1/2), and p38 are the main signaling intermediaries in the MAPK pathway and are involved in the anti-inflammatory activity of pyxinol [26]. The impact of 5c on the LPS-activated MAPK pathway was then assessed. LPS was observed to activate the MAPK pathway via a marked upregulation of JNK, ERK1/2, and p38 phosphorylation. On the contrary, 5c inhibited this upregulation of JNK and p38 phosphorylation in a concentration-dependent manner. However, 5c did not inhibit the upregulation of ERK1/2 phosphorylation (Figure 6B). Our previous study indicated that pyxinol derivatives could only inhibit the LPS-induced upregulation of ERK1/2 and p38 phosphorylation [26]. Other ginsenosides have also been reported to selectively

modulate JNK phosphorylation to suppress inflammation [6,36]. The data suggest that these signaling intermediaries of MAPK may interact with these compounds and that the dehydrogenation at C-12 may greatly affect this interaction. This issue needs to be resolved in the future. In summary, compound **5c** exhibited its anti-inflammatory activity via the inhibition of JNK and p38 activation.

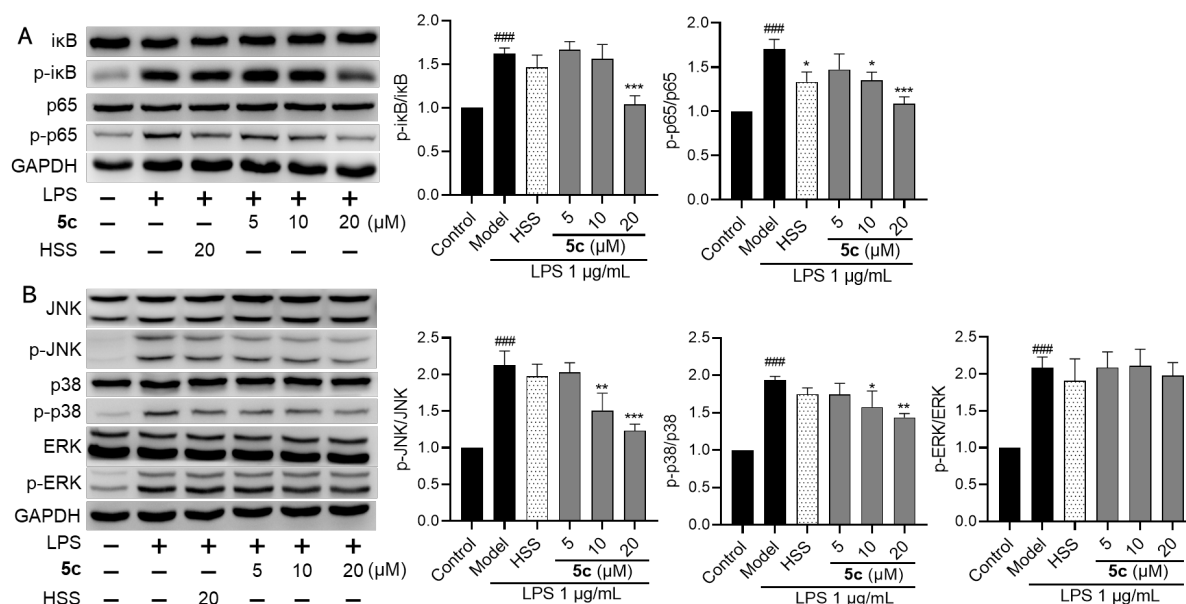


Figure 6. The impact of compound **5c** on LPS-triggered (A) NF-κB and (B) MAPK (JNK, p38, and ERK1/2) activation in RAW264.7 macrophages following a 2 h treatment with a combination of LPS (1 μg/mL) and **5c** or HSS. Data are expressed as the means ± SD ($n = 3$) from triplicate experiments. ### $p < 0.001$ vs. control; * $p < 0.05$, ** $p < 0.01$, *** $p < 0.001$ vs. model.

2.5. The GR-Independent Effect of **5c** on Its Anti-Inflammatory Activity

GCs are well-known anti-inflammatory drugs in clinical settings that regulate anti-inflammation by activating the GC receptor (GR). Previous studies have reported that the activation of GR signaling is involved in the anti-inflammatory activity of ginsenosides [10,37]. Whether the anti-inflammatory activity of **5c** was related to the activation of GR signaling was assessed next. As expected, the inhibitory effect of HSS on LPS-triggered NO production was completely blocked by RU-486, a specific GR antagonist, whereas the NO inhibition effect of **5c** was not impacted by it (Figure 7A). Similar results were observed for other 12-dehydroxyxynol derivatives. To further confirm whether an in situ interaction existed between GR and **5c**, the cellular thermal shift assay (CETSA) was performed. CETSA is a powerful label-free method used to analyze protein–compound interactions in physiological environments. Such interactions in situ can increase/decrease a protein’s overall resistance to thermal denaturation, thereby resulting in the amount change of the protein in the soluble lysate fraction at a high temperature [38,39]. Briefly, RAW264.7 cells were incubated with either **5c** (20 μM) or HSS (20 μM), followed by thermal denaturation at indicated temperatures. Then, the cells were lysed with freeze–thaw cycles, and soluble fractions were collected and evaluated using Western blotting. Compared with DMSO-treatment, HSS-treatment stabilized GR at high temperatures, which proves the expected interactions between GR and HSS (Figure 7B). In contrast, **5c**-treatment did not exhibit any detectable differences from DMSO-treatment at the same conditions. Molecular docking analysis also suggested that HSS had a strong binding affinity for GR; however, **5c** did not have this affinity (data not shown). These results strongly imply that **5c** exerts its anti-inflammatory activity in GR-independent ways.

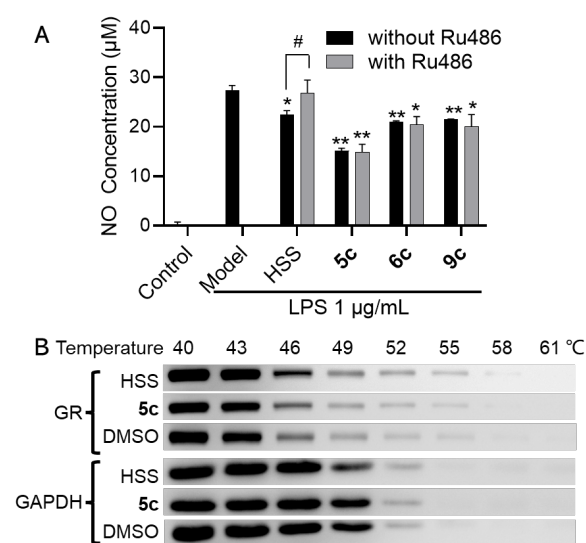


Figure 7. The GR-independent effect of derivative **5c** on its anti-inflammatory activity: **(A)** Effect of Ru486 (a specific GR antagonist) on the NO inhibitory effects of 12-dehydropyxinol derivatives. After pretreatment with the test compounds (20 µM) in the presence or absence of Ru486 (10 µM) for 2 h, the macrophages were treated with LPS (1 µg/mL) for another 24 h. Data are expressed as the means ± SD ($n = 3$): * $p < 0.05$, ** $p < 0.01$ vs. model; # $p < 0.05$ vs. without Ru486 group. **(B)** CESTA assessment of derivative **5c** in RAW264.7 macrophages. Immunoblotting results for GR thermal aggregation curves from samples treated with **5c** (20 µM), HSS (20 µM), or DMSO as a control.

3. Materials and Methods

3.1. Chemistry

The experimental reagents were obtained from commercial sources and the synthesized compounds were purified using 200–300 mesh-silica gel column chromatography. ^1H and ^{13}C NMR analyses were performed on a JEOL-ECA400 spectrometer. Chemical shifts (δ) were given as p.p.m. relative to tetramethylsilane (^1H : 0.0 p.p.m.) in CDCl_3 (^{13}C : 77.0 p.p.m.) or CD_2HOD in CD_3OD (^1H : 3.30 p.p.m., ^{13}C : 49.0 p.p.m.). Thermo Scientific Q Exactive and SGW-3 apparatuses were, respectively, used to determine high-resolution mass-spectra (HRMS) and optical rotation.

The Synthesis of **5a–5f**, **6a–6f**, **9a–9f** and **10a–10f**

Pyxinol (**1**), 24*S*-pyxinol (**2**), and the intermediates (**3–4**) were prepared following published procedures [16,27,29].

To the mixture of **1** or **2** (44.0 mg, 0.0922 mmol) and NaHCO_3 (46.4 mg, 0.553 mmol) in dehydrated CH_2Cl_2 (2.0 mL) was added Dess–Martin reagent (196 mg, 0.461 mmol) and *tert*-BuOH at 0 °C. Subsequent to stirring for 6 h at rt, Na_2SO_3 aq. was added to the mixture and extracted with EtOAc, dried over Na_2SO_4 , and purified using column chromatography ($V_{\text{petroleum ether}}: V_{\text{ethyl acetate}} = 10:1-5:1-4:1$) to produce **3** or **7** (over 95%).

To **3** or **7** (31 mg, 0.065 mmol) in *i*PrOH (1.2 mL), NaBH_4 (6 mg, 0.16 mmol) was added at 0 °C under argon. Subsequent to stirring for 1 h, sat. NH_4Cl aq. was added to the reaction mixture and extracted with EtOAc, dried over Na_2SO_4 , and purified using column chromatography ($V_{\text{petroleum ether}}: V_{\text{ethyl acetate}} = 8:1-4:1-3:1$) to produce **4** or **8** (over 95%).

To the mixture of **4** or **8** (20 mg, 0.042 mmol), *N*-Boc amino acid (*L*-*N*-Boc-Methionine, *L*-*N*-Boc-Valine, *L*-*N*-Boc-Phenylalanine, *L*-*N*-Boc-*O*-Bz-Threonine, *N*-Boc-Glycine, or *L*-*N*-Boc-*O*-*t*Bu-Aspartic acid) (0.064 mmol) and EDCI (32 mg, 0.167 mmol) in dehydrated CH_2Cl_2 (1.2 mL), DMAP (1 mg, 0.008 mmol) was added at 0 °C under argon. Subsequent to stirring for 1 d at rt, water was added to the reaction mixture and extracted with CH_2Cl_2 , dried over Na_2SO_4 , and purified using column chromatography ($V_{\text{petroleum ether}}: V_{\text{ethyl acetate}}$) to produce **5a–5f** and **9a–9f**.

TFA (1.2 mL) was added into **5a** (**5b**, **5c**, **5d**, **5e**, **5f**, **9a**, **9b**, **9c**, **9d**, **9e**, or **9f**) (0.03 mmol) at 0 °C. Subsequent to stirring at rt for 15 min, the solution was concentrated in vacuo to produce **6a–6f** and **10a–10f** (Supplementary Material).

Compound **5a**, yield: 92%. $[\alpha]_D^{21} + 19.4$ (c 1.0, CHCl₃); ¹H NMR (400 MHz, CDCl₃) δ 5.11 (d, J = 7.7 Hz, 1H, -NH-), 4.52 (dd, J = 11.0, 5.2 Hz, 1H, -COOCH-), 4.42–4.37 (m, 1H, -OCOCH-), 3.70 (dd, J = 8.4, 6.2 Hz, 1H, -OCH-), 2.90 (d, J = 9.3 Hz, 1H, -COCH-), 2.60–2.51 (m, 3H), 2.20 (d, J = 8.2 Hz, 2H), 2.14 (dd, J = 10.4, 8.0 Hz, 1H), 2.10 (s, 3H, -SCH₃), 1.95–0.80 (m, 20H), 1.44 (s, 9H, -C(CH₃)₃), 1.21 (s, 3H, -CH₃), 1.20 (s, 3H, -CH₃), 1.11 (s, 6H, -CH₃ × 2), 0.96 (s, 3H, -CH₃), 0.89 (s, 3H, -CH₃), 0.87 (s, 3H, -CH₃), 0.76 (s, 3H, -CH₃). ¹³C NMR (100 MHz, CDCl₃) δ 211.2, 171.9, 155.3, 85.2, 83.6, 81.9, 79.9, 71.1, 57.0, 55.8, 55.7, 54.1, 53.2, 42.6, 40.4, 39.7, 38.1, 38.0, 37.5, 35.1, 34.1, 32.5, 32.0, 28.3 (3C), 28.1, 28.0, 27.6, 26.5, 25.6, 25.0, 24.4, 23.5, 18.2, 16.6, 16.5, 16.0, 15.6, 15.5. HRMS (ESI) *m/z* calcd C₄₀H₆₇NO₇SNa⁺ [M + Na]⁺ 728.4530, found 728.4525.

Compound **5b**, yield: 72%. $[\alpha]_D^{22} + 31.1$ (c 1.0, CHCl₃); ¹H NMR (400 MHz, CDCl₃) δ 5.00 (d, J = 9.3 Hz, 1H, -NH-), 4.51 (dd, J = 11.4, 4.8 Hz, 1H, -COOCH-), 4.22 (dd, J = 9.1, 4.1 Hz, 1H, -OCOCH-), 3.69 (dd, J = 8.5, 6.0 Hz, 1H, -OCH-), 2.90 (d, J = 9.6 Hz, 1H, -COCH-), 2.57 (td, J = 10.2, 4.1 Hz, 1H, -COCHCHCH₂-), 2.22–2.16 (m, 3H), 1.87–0.85 (m, 18H), 1.44 (s, 9H, -C(CH₃)₃), 1.21 (s, 3H, -CH₃), 1.20 (s, 3H, -CH₃), 1.11 (s, 3H, -CH₃), 1.10 (s, 3H, -CH₃), 0.99 (d, J = 6.9 Hz, 3H, -CH-CH₃), 0.96 (s, 3H, -CH₃), 0.89 (s, 3H, -CH₃), 0.88 (d, J = 7.1 Hz, 3H, -CH-CH₃), 0.87 (s, 3H, -CH₃), 0.76 (s, 3H, -CH₃). ¹³C NMR (100 MHz, CDCl₃) δ 211.2, 172.0, 155.7, 85.1, 83.6, 81.6, 79.6, 71.1, 58.8, 57.0, 55.8, 55.7, 54.1, 42.6, 40.4, 39.7, 38.1, 37.9, 37.5, 35.1, 34.1, 32.0, 31.2, 28.3 (3C), 28.0, 27.6, 26.5, 25.6, 25.0, 24.4, 23.5, 19.3, 18.2, 17.2, 16.6, 16.6, 16.0, 15.6. HRMS (ESI) *m/z* calcd C₄₀H₆₇NO₇Na⁺ [M + Na]⁺ 696.4810, found 696.4787.

Compound **5c**, yield: 83%. $[\alpha]_D^{27} + 37.3$ (c 1.0, CHCl₃); ¹H NMR (400 MHz, CDCl₃) δ 7.31–7.16 (m, 5H, Ar-H × 5), 4.90 (d, J = 8.5 Hz, 1H, -NH-), 4.56 (q, J = 7.0 Hz, 1H, -OCOCH-), 4.48 (dd, J = 11.4, 4.5 Hz, 1H, -COOCH-), 3.69 (dd, J = 8.7, 6.2 Hz, 1H, -OCH-), 3.12 (dd, J = 13.9, 5.9 Hz, 1H, PhCH_a-), 3.01 (dd, J = 13.9, 6.7 Hz, 1H, PhCH_b-), 2.89 (d, J = 9.3 Hz, 1H, -COCH-), 2.56 (td, J = 10.0, 4.1 Hz, 1H, -COCHCHCH₂-), 2.27–2.12 (m, 2H), 1.89–0.80 (m, 18H), 1.39 (s, 9H, -C(CH₃)₃), 1.21 (s, 3H, -CH₃), 1.19 (s, 3H, -CH₃), 1.11 (s, 3H, -CH₃), 1.10 (s, 3H, -CH₃), 0.93 (s, 3H, -CH₃), 0.81 (s, 3H, -CH₃), 0.78 (s, 3H, -CH₃), 0.76 (s, 3H, -CH₃); ¹³C NMR (100 MHz, CDCl₃) δ 211.2, 171.8, 155.1, 136.1, 129.3 (2C), 128.5 (2C), 126.9, 85.1, 83.6, 81.9, 79.8, 71.1, 57.0, 55.8, 55.7, 54.6, 54.1, 42.6, 40.4, 39.7, 38.5, 38.2, 37.9, 37.5, 35.1, 34.1, 32.0, 28.3 (3C), 27.9, 27.6, 26.5, 25.6, 25.0, 24.4, 23.3, 18.2, 16.6, 16.4, 16.0, 15.6. HRMS (ESI) *m/z* calcd C₄₄H₆₇NO₇Na⁺ [M + Na]⁺ 744.4810, found 744.4779.

Compound **5d**, yield: 85%. $[\alpha]_D^{22} + 22.4$ (c 1.00, CHCl₃); ¹H NMR (400 MHz, CDCl₃) δ 7.33–7.24 (m, 5H, Ar-H × 5), 5.27 (d, J = 9.9 Hz, 1H, -NH-), 4.55 (d, J = 11.0 Hz, 1H, PhCH_a-), 4.53 (dd, J = 12.1, 4.4 Hz, 1H, -COOCH-), 4.38 (d, J = 11.3 Hz, 1H, PhCH_b-), 4.29 (dd, J = 9.8, 2.1 Hz, 1H, -OCOCH-), 4.20 (qd, J = 6.2, 2.0 Hz, 1H, PhCH₂OCH-), 3.69 (dd, J = 8.4, 6.2 Hz, 1H, -OCH-), 2.89 (d, J = 9.6 Hz, 1H, -COCH-), 2.57 (td, J = 10.0, 4.1 Hz, 1H, -COCHCHCH₂-), 2.21–2.15 (m, 2H), 1.99 (br, 1H), 1.86–1.02 (m, 17H), 1.45 (s, 9H, -C(CH₃)₃), 1.29 (d, J = 6.3 Hz, 3H, -CHCH₃), 1.21 (s, 3H, -CH₃), 1.19 (s, 3H, -CH₃), 1.11 (s, 3H, -CH₃), 1.10 (s, 3H, -CH₃), 0.94 (s, 3H, -CH₃), 0.87 (s, 3H, -CH₃), 0.82 (s, 3H, -CH₃), 0.76 (s, 3H, -CH₃). ¹³C NMR (100 MHz, CDCl₃) δ 211.2, 170.9, 156.0, 137.9, 128.2 (2C), 127.6, 127.4 (2C), 85.1, 83.5, 81.7, 79.7, 75.4, 71.1, 70.9, 58.6, 57.0, 55.7, 55.6, 54.0, 42.5, 40.4, 39.7, 38.2, 37.9, 37.5, 35.1, 34.1, 32.0, 28.3 (3C), 27.9, 27.6, 26.5, 25.6, 24.9, 24.4, 23.4, 18.2, 16.6, 16.5, 16.4, 16.0, 15.6. HRMS (ESI) *m/z* calcd C₄₆H₇₁NO₈Na⁺ [M + Na]⁺ 788.5072, found 788.5042.

Compound **5e**, yield: 79%. $[\alpha]_D^{30} + 21.3$ (c 1.0, CHCl₃); ¹H NMR (400 MHz, CDCl₃) δ 5.01 (s, 1H, -NH-), 4.54 (dd, J = 11.2, 5.3 Hz, 1H, -COOCH-), 3.90 (d, J = 5.0 Hz, 2H, -OCOCH₂NHBoc), 3.70 (dd, J = 8.7, 5.9 Hz, 1H, -OCH-), 2.89 (d, J = 9.6 Hz, 1H, -COCH-), 2.57 (td, J = 10.1, 4.3 Hz, 1H, -COCHCHCH₂-), 2.27–2.09 (m, 2H), 1.90–0.80 (m, 18H), 1.45 (s, 9H, -C(CH₃)₃), 1.21 (s, 3H, -CH₃), 1.20 (s, 3H, -CH₃), 1.11 (s, 3H, -CH₃), 1.10 (s, 3H, -CH₃), 0.95 (s, 3H, -CH₃), 0.87 (s, 3H, -CH₃), 0.87 (s, 3H, -CH₃), 0.76 (s, 3H, -CH₃); ¹³C NMR (100 MHz, CDCl₃) δ 211.3, 170.0, 155.6, 85.2, 83.5, 81.7, 79.9, 71.2, 57.0, 55.7, 55.7, 54.1, 42.6, 42.6, 40.4, 39.7, 38.2, 38.0, 37.5, 35.1, 34.1, 32.0, 28.3 (3C), 28.0, 27.6, 26.5, 25.6, 25.0, 24.3,

23.4, 18.2, 16.6, 16.4, 16.1, 15.6. HRMS (ESI) m/z calcd $C_{37}H_{61}NO_7Na^+$ $[M + Na]^+$ 654.4340, found 654.4316.

Compound **5f**, yield: 80%. $[\alpha]_D^{30} + 34.7$ (c 1.0, $CHCl_3$); 1H NMR (400 MHz, $CDCl_3$) δ 5.54 (d, $J = 8.8$ Hz, 1H, $-NH-$), 4.52–4.47 (m, 2H), 3.69 (dd, $J = 8.7, 6.2$ Hz, 1H, $-OCH-$), 2.94–2.88 (m, 2H), 2.73 (dd, $J = 17.0, 4.4$ Hz, 1H, $-CH_2COOtBu$), 2.56 (td, $J = 10.1, 4.2$ Hz, 1H, $-COCHCHCH_2-$), 2.23–2.19 (m, 2H), 1.89–0.86 (m, 18H), 1.45 (s, 9H, $-C(CH_3)_3$), 1.43 (s, 9H, $-C(CH_3)_3$), 1.21 (s, 3H, $-CH_3$), 1.19 (s, 3H, $-CH_3$), 1.11 (s, 3H, $-CH_3$), 1.10 (s, 3H, $-CH_3$), 0.95 (s, 3H, $-CH_3$), 0.87 (s, 3H, $-CH_3$), 0.86 (s, 3H, $-CH_3$), 0.76 (s, 3H, $-CH_3$); ^{13}C NMR (100 MHz, $CDCl_3$) δ 211.2, 170.9, 170.3, 155.5, 85.1, 83.5, 81.9, 81.6, 79.8, 71.1, 57.0, 55.8, 55.7, 54.0, 50.2, 42.5, 40.4, 39.7, 38.1, 37.9, 37.7, 37.5, 35.1, 34.1, 32.0, 28.3 (3C), 28.0 (3C), 28.0, 27.6, 26.5, 25.6, 24.9, 24.4, 23.3, 18.2, 16.6, 16.5, 16.0, 15.6. HRMS (ESI) m/z calcd $C_{43}H_{71}NO_9Na^+$ $[M + Na]^+$ 768.5021, found 768.4998.

Compound **6a**, yield: 90%. $[\alpha]_D^{21} + 38.9$ (c 0.50, CH_3OH); 1H NMR (400 MHz, CD_3OD) δ 4.65 (dd, $J = 10.0, 6.5$ Hz, 1H, $-COOCH-$), 4.21 (t, $J = 6.2$ Hz, 1H, $-OCOCH-$), 3.72 (t, $J = 7.1$ Hz, 1H, $-OCH-$), 3.04 (d, $J = 9.6$ Hz, 1H, $-COCH-$), 2.67 (t, $J = 7.4$ Hz, 2H, $-SCH_2-$), 2.51 (td, $J = 10.0, 4.4$ Hz, 1H, $-COCHCHCH_2-$), 2.36 (t, $J = 13.2$ Hz, 1H, $-COCH_aCH-$), 2.31–2.22 (m, 1H), 2.16–2.09 (m, 4H), 2.11 (s, 3H, $-SCH_3$), 1.93–0.87 (m, 16H), 1.26 (s, 3H, $-CH_3$), 1.11 (s, 3H, $-CH_3$), 1.11 (s, 3H, $-CH_3$), 1.09 (s, 3H, $-CH_3$), 1.02 (s, 3H, $-CH_3$), 0.95 (s, 3H, $-CH_3$), 0.92 (s, 3H, $-CH_3$), 0.77 (s, 3H, $-CH_3$). ^{13}C NMR (100 MHz, CD_3OD) δ 214.3, 170.3, 86.6, 85.2, 85.0, 72.7, 58.2, 57.1, 56.9, 55.7, 53.0, 43.9, 41.8, 40.7, 39.2, 39.1, 38.7, 35.5, 35.3, 33.1, 30.9, 30.1, 28.6, 27.5, 26.2, 26.0, 25.8, 25.4, 24.4, 19.3, 17.1, 17.0, 16.5, 16.1, 14.9. HRMS (ESI) m/z calcd $C_{35}H_{59}NO_5SNa^+$ $[M + Na]^+$ 628.4007, found 628.3995.

Compound **6b**, yield: 90%. $[\alpha]_D^{26} + 29.6$ (c 1.0, $CHCl_3$); 1H NMR (400 MHz, $CDCl_3$) δ 4.59 (dd, $J = 10.7, 3.8$ Hz, 1H, $-COOCH-$), 3.88–3.83 (m, 1H), 3.74 (t, $J = 7.1$ Hz, 1H, $-OCH-$), 2.87 (d, $J = 9.6$ Hz, 1H, $-COCH-$), 2.57 (td, $J = 9.7, 4.0$ Hz, 1H, $-COCHCHCH_2-$), 2.39–2.30 (m, 1H), 2.25–2.15 (m, 2H), 1.91–0.81 (m, 18H), 1.26 (s, 3H, $-CH_3$), 1.20 (s, 6H, $-CH_3 \times 2$), 1.11 (s, 3H, $-CH_3$), 1.09 (d, $J = 6.6$ Hz, 3H, $-CHCH_3$), 1.07 (s, 3H, $-CH_3$), 0.95 (s, 3H, $-CH_3$), 0.88 (s, 3H, $-CH_3$), 0.89 (d, $J = 6.6$ Hz, 3H, $-CHCH_3$), 0.77 (s, 3H, $-CH_3$). ^{13}C NMR (100 MHz, $CDCl_3$) δ 211.8, 167.7, 85.3, 83.9, 83.5, 71.3, 58.7, 57.0, 55.7, 55.6, 54.0, 42.4, 40.4, 39.6, 38.0, 37.8, 37.4, 34.4, 34.1, 32.0, 31.9, 28.1, 27.5, 26.9, 26.5, 25.6, 25.2, 23.6, 18.2, 18.0, 17.5, 16.8, 16.6, 15.9, 15.6. HRMS (ESI) m/z calcd $C_{35}H_{59}NO_5Na^+$ $[M + Na]^+$ 596.4285, found 596.4260.

Compound **6c**, yield: 90%. $[\alpha]_D^{26} + 30.0$ (c 1.0, $CHCl_3$); 1H NMR (400 MHz, $CDCl_3$) δ 7.34–7.24 (m, 5H, $Ar-H \times 5$), 4.50–4.46 (m, 1H), 4.22 (dd, $J = 11.3, 5.5$ Hz, 1H, $PhCH_2CH-$), 3.72 (t, $J = 6.7$ Hz, 1H, $-OCH-$), 3.30–3.25 (m, 2H), 2.86 (d, $J = 9.3$ Hz, 1H, $-COCH-$), 2.56 (td, $J = 9.3, 2.4$ Hz, 1H, $-COCHCHCH_2-$), 2.18–2.16 (m, 2H), 1.90–0.66 (m, 18H), 1.19 (s, 3H, $-CH_3$), 1.18 (s, 3H, $-CH_3$), 1.11 (s, 3H, $-CH_3$), 1.07 (s, 3H, $-CH_3$), 0.91 (s, 3H, $-CH_3$), 0.76 (s, 3H, $-CH_3$), 0.73 (s, 3H, $-CH_3$), 0.71 (s, 3H, $-CH_3$). ^{13}C NMR (100 MHz, $CDCl_3$) δ 211.7, 168.8, 133.6, 129.3 (2C), 129.2 (2C), 127.9, 85.3, 84.1, 83.5, 71.4, 57.0, 55.7, 55.7, 54.3, 54.0, 42.5, 40.4, 39.6, 38.0, 37.7, 37.4, 36.5, 34.6, 34.1, 31.9, 27.9, 27.6, 26.9, 26.6, 25.6, 25.1, 23.8, 18.1, 16.6, 16.2, 16.0, 15.6. HRMS (ESI) m/z calcd $C_{39}H_{59}NO_5Na^+$ $[M + Na]^+$ 644.4285, found 644.4258.

Compound **6d**, yield: 90%. $[\alpha]_D^{22} + 18.7$ (c 1.00, CH_3OH); 1H NMR (400 MHz, CD_3OD) δ 7.36–7.26 (m, 5H, $Ar-H \times 5$), 4.69 (d, $J = 11.5$ Hz, 1H, $PhCH_a-$), 4.62 (dd, $J = 10.6, 4.5$ Hz, 1H, $-COOCH-$), 4.46 (d, $J = 11.5$ Hz, 1H, $PhCH_b-$), 4.29 (qd, $J = 6.3, 3.0$ Hz, 1H, $PhCH_2OCH-$), 4.13 (d, $J = 2.7$ Hz, 1H, $-OCOCH-$), 3.72 (dd, $J = 8.9, 5.4$ Hz, 1H, $-OCH-$), 3.03 (d, $J = 9.3$ Hz, 1H, $-COCH-$), 2.51 (td, $J = 9.8, 4.3$ Hz, 1H, $-COCHCHCH_2-$), 2.35 (t, $J = 13.2$ Hz, 1H, $-COCH_aCH-$), 2.12 (dd, $J = 12.9, 3.6$ Hz, 1H, $-COCH_bCH-$), 1.92–0.90 (m, 18H), 1.42 (d, $J = 6.3$ Hz, 3H, $-CHCH_3$), 1.25 (s, 3H, $-CH_3$), 1.11 (s, 3H, $-CH_3$), 1.11 (s, 3H, $-CH_3$), 1.09 (s, 3H, $-CH_3$), 1.01 (s, 3H, $-CH_3$), 0.93 (s, 3H, $-CH_3$), 0.82 (s, 3H, $-CH_3$), 0.76 (s, 3H, $-CH_3$). ^{13}C NMR (100 MHz, CD_3OD) δ 214.3, 168.8, 138.8, 129.4 (2C), 128.9, 128.8 (2C), 86.6, 85.2, 85.0, 74.0, 72.7, 72.0, 59.2, 58.2, 57.0, 56.9, 55.7, 43.9, 41.7, 40.7, 39.2, 39.0, 38.7, 35.5, 35.2, 33.0, 28.7, 27.5, 26.2, 26.0, 25.8, 25.5, 24.4, 19.3, 17.1, 17.0, 16.5, 16.4, 16.1. HRMS (ESI) m/z calcd $C_{41}H_{64}NO_6^+$ $[M + H]^+$ 666.4728, found 666.4700.

Compound **6e**, yield: 90%. $[\alpha]_D^{26} + 14.5$ (c 1.0, $CHCl_3$); 1H NMR (400 MHz, CD_3OD) δ 4.64 (dd, $J = 10.9, 5.9$ Hz, 1H, $-COOCH-$), 3.83 (d, $J = 17.3$ Hz, 1H, $-OCOCH_a-$), 3.77 (d,

$J = 17.3$ Hz, 1H, -OCOCH_b-), 3.72 (t, $J = 7.1$ Hz, 1H, -OCH-), 3.04 (d, $J = 9.6$ Hz, 1H, -COCH-), 2.51 (td, $J = 10.0, 4.2$ Hz, 1H, -COCHCH₂-), 2.36 (t, $J = 13.3$ Hz, 1H, -COCH_aCH-), 2.12 (dd, $J = 13.1, 3.7$ Hz, 1H, -COCH_bCH-), 1.91–0.85 (m, 18H), 1.25 (s, 3H, -CH₃), 1.12 (s, 3H, -CH₃), 1.11 (s, 3H, -CH₃), 1.09 (s, 3H, -CH₃), 1.02 (s, 3H, -CH₃), 0.93 (s, 3H, -CH₃), 0.92 (s, 3H, -CH₃), 0.77 (s, 3H, -CH₃). ¹³C NMR (100 MHz, CD₃OD) δ 214.3, 165.0, 86.6, 85.2, 85.2, 72.7, 58.2, 57.1, 57.0, 55.8, 43.9, 41.8, 40.7, 40.6, 39.3, 39.1, 38.7, 35.6, 35.3, 33.1, 28.4, 27.5, 26.2, 26.0, 25.7, 25.4, 24.5, 19.3, 17.1, 16.8, 16.6, 16.1. HRMS (ESI) m/z calcd C₃₂H₅₃NO₅Na⁺ [M + Na]⁺ 554.3816, found 554.3795.

Compound **6f**, yield: 90%. [α]_D³⁰ + 30.1 (c 1.0, CHCl₃); ¹H NMR (400 MHz, CD₃OD) δ 4.63 (dd, $J = 11.0, 5.2$ Hz, 1H, -COOCH-), 4.29 (dd, $J = 12.9, 6.0$ Hz, 1H, -OCOCH-), 3.72 (t, $J = 7.1$ Hz, 1H, -OCH-), 3.09–2.94 (m, 3H), 2.51 (td, $J = 9.8, 4.2$ Hz, 1H, -COCHCH₂-), 2.36 (t, $J = 13.3$ Hz, 1H, -COCH_aCH-), 2.12 (dd, $J = 12.9, 3.6$ Hz, 1H, -COCH_bCH-), 1.92–0.95 (m, 18H), 1.25 (s, 3H, -CH₃), 1.11 (s, 3H, -CH₃), 1.11 (s, 3H, -CH₃), 1.09 (s, 3H, -CH₃), 1.01 (s, 3H, -CH₃), 0.93 (s, 3H, -CH₃), 0.89 (s, 3H, -CH₃), 0.77 (s, 3H, -CH₃). ¹³C NMR (100 MHz, CD₃OD) δ 214.3, 172.6, 169.2, 86.6, 85.2, 85.0, 72.7, 58.2, 57.1, 57.0, 55.7, 50.8, 43.9, 41.8, 40.7, 39.2, 39.1, 38.7, 35.5, 35.3, 34.6, 33.0, 28.4, 27.5, 26.2, 26.0, 25.8, 25.4, 24.4, 19.3, 17.1, 16.9, 16.5, 16.1. HRMS (ESI) m/z calcd C₃₄H₅₅NO₇Na⁺ [M + Na]⁺ 612.3871, found 612.3845.

Compound **9a**, yield: 87%. [α]_D²⁰ + 30.0 (c 1.00, CHCl₃); ¹H NMR (400 MHz, CDCl₃) δ 5.11 (d, $J = 8.0$ Hz, 1H, -NH-), 4.52 (dd, $J = 11.0, 5.2$ Hz, 1H, -COOCH-), 4.40 (dd, $J = 12.2, 8.4$ Hz, 1H, -OCOCH-), 3.71 (dd, $J = 9.8, 5.6$ Hz, 1H, -OCH-), 2.96 (d, $J = 9.6$ Hz, 1H, -COCH-), 2.59–2.51 (m, 3H), 2.22–2.12 (m, 4H), 2.10 (s, 3H, -SCH₃), 1.95–0.85 (m, 18H), 1.45 (s, 9H, -C(CH₃)₃), 1.21 (s, 3H, -CH₃), 1.19 (s, 3H, -CH₃), 1.09 (s, 3H, -CH₃), 1.04 (s, 3H, -CH₃), 0.97 (s, 3H, -CH₃), 0.90 (s, 3H, -CH₃), 0.87 (s, 3H, -CH₃), 0.75 (s, 3H, -CH₃). ¹³C NMR (100 MHz, CDCl₃) δ 210.8, 171.9, 155.3, 87.5, 85.2, 81.9, 79.9, 70.3, 57.2, 55.9, 55.8, 54.2, 53.2, 43.0, 40.4, 39.6, 38.1, 38.0, 37.5, 36.5, 34.2, 32.5, 31.9, 30.0, 28.3 (3C), 28.1, 27.7, 26.6, 26.2, 24.8, 23.9, 23.4, 18.2, 16.5 (2C), 16.1, 15.6, 15.5. HRMS (ESI) m/z calcd C₄₀H₆₇NO₇Na⁺ [M + Na]⁺ 728.4530, found 728.4501.

Compound **9b**, yield: 88%. [α]_D²⁴ + 26.4 (c 1.0, CHCl₃); ¹H NMR (400 MHz, CDCl₃) δ 5.01 (d, $J = 9.1$ Hz, 1H, -NH-), 4.51 (dd, $J = 11.5, 4.9$ Hz, 1H, -COOCH-), 4.22 (dd, $J = 9.2, 4.3$ Hz, 1H, -OCOCH-), 3.71 (dd, $J = 9.8, 5.6$ Hz, 1H, -OCH-), 2.96 (d, $J = 9.3$ Hz, 1H, -COCH-), 2.54 (td, $J = 9.9, 4.2$ Hz, 1H, -COCHCH₂-), 2.22–2.14 (m, 2H), 1.95–1.51 (m, 19H), 1.45 (s, 9H, -C(CH₃)₃), 1.21 (s, 3H, -CH₃), 1.19 (s, 3H, -CH₃), 1.09 (s, 3H, -CH₃), 1.04 (s, 3H, -CH₃), 0.99 (d, $J = 6.9$ Hz, 3H, -CHCH₃), 0.97 (s, 3H, -CH₃), 0.90 (s, 3H, -CH₃), 0.88 (d, $J = 7.15$ Hz, 3H, -CHCH₃), 0.88 (s, 3H, -CH₃), 0.75 (s, 3H, -CH₃). ¹³C NMR (100 MHz, CDCl₃) δ 210.9, 172.0, 155.7, 87.5, 85.3, 81.6, 79.6, 70.3, 58.8, 57.2, 55.9, 55.8, 54.2, 43.0, 40.4, 39.6, 38.2, 37.9, 37.5, 36.5, 34.2, 31.9, 31.2, 28.3 (3C), 28.0, 27.7, 26.6, 26.2, 24.8, 23.9, 23.5, 19.3, 18.2, 17.1, 16.6 (2C), 16.0, 15.6. HRMS (ESI) m/z calcd C₄₀H₆₇NO₇Na⁺ [M + Na]⁺ 696.4810, found 696.4782.

Compound **9c**, yield: 93%. [α]_D²⁴ + 25.2 (c 1.0, CHCl₃); ¹H NMR (400 MHz, CDCl₃) δ 7.31–7.27 (m, 2H, Ar-H \times 2), 7.23 (tt, $J = 7.2, 1.6$ Hz, 1H, Ar-H), 7.17 (dd, $J = 8.0, 1.4$ Hz, 2H, Ar-H \times 2), 4.89 (d, $J = 8.8$ Hz, 1H, -NH-), 4.57 (q, $J = 6.8$ Hz, 1H, -OCOCH-), 4.48 (dd, $J = 11.4, 4.5$ Hz, 1H, -COOCH-), 3.71 (dd, $J = 9.9, 5.5$ Hz, 1H, -OCH-), 3.13 (dd, $J = 13.9, 5.9$ Hz, 1H, PhCH_a-), 3.02 (dd, $J = 13.7, 6.9$ Hz, 1H, PhCH_b-), 2.95 (d, $J = 9.3$ Hz, 1H, -COCH-), 2.54 (td, $J = 9.8, 4.1$ Hz, 1H, -COCHCH₂-), 2.22–2.18 (m, 2H), 1.95–0.79 (m, 18H), 1.39 (s, 9H, -C(CH₃)₃), 1.19 (s, 3H, -CH₃), 1.19 (s, 3H, -CH₃), 1.09 (s, 3H, -CH₃), 1.04 (s, 3H, -CH₃), 0.95 (s, 3H, -CH₃), 0.82 (s, 3H, -CH₃), 0.79 (s, 3H, -CH₃), 0.75 (s, 3H, -CH₃). ¹³C NMR (100 MHz, CDCl₃) δ 210.9, 171.8, 155.1, 136.1, 129.3 (2C), 128.5 (2C), 126.9, 87.6, 85.3, 81.9, 79.8, 70.3, 57.2, 55.9, 55.8, 54.6, 54.2, 43.0, 40.4, 39.6, 39.6, 38.2, 37.9, 37.5, 36.5, 34.2, 31.9, 28.3 (3C), 27.9, 27.7, 26.6, 26.2, 24.8, 23.9, 23.3, 18.2, 16.6, 16.4, 16.0, 15.6. HRMS (ESI) m/z calcd C₄₄H₆₇NO₇Na⁺ [M + Na]⁺ 744.4810, found 744.4781.

Compound **9d**, yield: 89%. [α]_D²¹ + 24.8 (c 1.00, CHCl₃); ¹H NMR (400 MHz, CDCl₃) δ 7.33–7.24 (m, 5H, Ar-H \times 5), 5.27 (d, $J = 9.6$ Hz, 1H, -NH-), 4.55 (d, $J = 11.0$ Hz, 1H, PhCH_a-), 4.53 (dd, $J = 11.3, 4.7$ Hz, 1H, -COOCH-), 4.38 (d, $J = 11.5$ Hz, 1H, PhCH_b-), 4.30 (dd, $J = 9.8, 2.1$ Hz, 1H, -OCOCH-), 4.21 (qd, $J = 6.1, 1.9$ Hz, 1H, PhCH₂OCH-), 3.71 (dd, $J = 9.8, 5.6$ Hz, 1H, -OCH-), 2.96 (d, $J = 9.3$ Hz, 1H, -COCH-), 2.54 (td, $J = 9.8, 4.1$ Hz, 1H, -COCHCH₂-),

2.21–2.19 (m, 2H), 2.09–2.08 (m, 1H), 1.93–0.82 (m, 17H), 1.45 (s, 9H, -C(CH₃)₃), 1.29 (d, J = 6.0 Hz, 3H, -CHCH₃), 1.20 (s, 3H, -CH₃), 1.19 (s, 3H, -CH₃), 1.09 (s, 3H, -CH₃), 1.04 (s, 3H, -CH₃), 0.95 (s, 3H, -CH₃), 0.87 (s, 3H, -CH₃), 0.82 (s, 3H, -CH₃), 0.75 (s, 3H, -CH₃). ¹³C NMR (100 MHz, CDCl₃) δ 210.9, 170.9, 156.0, 137.9, 128.2 (2C), 127.6, 127.4 (2C), 87.5, 85.2, 81.7, 79.7, 75.4, 70.8, 70.2, 58.6, 57.2, 55.8, 55.7, 54.2, 43.0, 40.4, 39.6, 38.2, 37.9, 37.5, 36.5, 34.2, 31.9, 28.3 (3C), 27.9, 27.7, 26.6, 26.2, 24.8, 23.9, 23.4, 18.2, 16.5 (2C), 16.4, 16.0, 15.6. HRMS (ESI) *m/z* calcd C₄₆H₇₁NO₈Na⁺ [M + Na]⁺ 788.5072, found 788.5043.

Compound **9e**, yield: 90%. [α]_D²⁴ + 38.6 (c 1.0, CHCl₃); ¹H NMR (400 MHz, CDCl₃) δ 5.01 (s, 1H, -NH-), 4.55 (dd, J = 11.3, 5.2 Hz, 1H, -COOCH-), 3.90 (d, J = 5.2 Hz, 2H, -OCOCH₂-), 3.71 (dd, J = 9.8, 5.6 Hz, 1H, -OCH-), 2.96 (d, J = 9.3 Hz, 1H, -COCH-), 2.54 (td, J = 9.8, 4.1 Hz, 1H, -COCHCHCH₂-), 2.26–2.20 (m, 2H), 1.95–1.08 (m, 18H), 1.45 (s, 9H, -C(CH₃)₃), 1.20 (s, 3H, -CH₃), 1.19 (s, 3H, -CH₃), 1.10 (s, 3H, -CH₃), 1.04 (s, 3H, -CH₃), 0.97 (s, 3H, -CH₃), 0.88 (s, 3H, -CH₃), 0.87 (s, 3H, -CH₃), 0.75 (s, 3H, -CH₃); ¹³C NMR (100 MHz, CDCl₃) δ 210.9, 170.0, 155.6, 87.6, 85.3, 81.7, 79.9, 70.3, 57.2, 55.9, 55.8, 54.2, 43.0, 42.6, 40.4, 39.6, 38.2, 38.0, 37.5, 36.5, 34.2, 31.9, 28.3 (3C), 28.0, 27.7, 26.7, 26.2, 24.8, 23.9, 23.4, 18.2, 16.6, 16.4, 16.1, 15.6. HRMS (ESI) *m/z* calcd C₃₇H₆₁NO₇Na⁺ [M + Na]⁺ 654.4340, found 654.4316.

Compound **9f**, yield: 89%. [α]_D²⁶ + 28.6 (c 1.0, CHCl₃); ¹H NMR (400 MHz, CDCl₃) δ 5.53 (d, J = 9.1 Hz, 1H, -NH-), 4.53–4.47 (m, 2H), 3.71 (dd, J = 9.9, 5.5 Hz, 1H, -OCH-), 2.96 (d, J = 9.3 Hz, 1H, -COCH-), 2.92 (dd, J = 17.0, 4.4 Hz, 1H, -CH_aCOOtBu), 2.73 (dd, J = 17.0, 4.4 Hz, 1H, -CH_bCOOtBu), 2.54 (td, J = 10.0, 4.0 Hz, 1H, -COCHCHCH₂-), 2.22–2.18 (m, 2H), 1.93–0.82 (m, 18H), 1.45 (s, 9H, -C(CH₃)₃), 1.43 (s, 9H, -C(CH₃)₃), 1.20 (s, 3H, -CH₃), 1.19 (s, 3H, -CH₃), 1.09 (s, 3H, -CH₃), 1.04 (s, 3H, -CH₃), 0.97 (s, 3H, -CH₃), 0.88 (s, 3H, -CH₃), 0.86 (s, 3H, -CH₃), 0.75 (s, 3H, -CH₃). ¹³C NMR (100 MHz, CDCl₃) δ 210.9, 170.9, 170.3, 155.5, 87.6, 85.3, 82.0, 81.6, 79.8, 70.3, 57.2, 55.9, 55.8, 54.2, 50.2, 43.0, 40.4, 39.7, 38.2, 38.0, 37.7, 37.5, 36.6, 34.2, 31.9, 28.3 (3C), 28.1 (3C), 28.0, 27.7, 26.6, 26.2, 24.8, 23.9, 23.3, 18.2, 16.6, 16.5, 16.1, 15.6. HRMS (ESI) *m/z* calcd C₄₃H₇₁NO₉Na⁺ [M + Na]⁺ 768.5021, found 768.4992.

Compound **10a**, yield: 91%. [α]_D²⁰ + 35.9 (c 1.00, CH₃OH); ¹H NMR (400 MHz, CD₃OD) δ 4.65 (dd, J = 10.4, 6.0 Hz, 1H, -COOCH-), 4.21 (dd, J = 7.0, 5.6 Hz, 1H, -OCOCH-), 3.70 (dd, J = 8.9, 6.7 Hz, 1H, -OCH-), 3.07 (d, J = 9.6 Hz, 1H, -COCH-), 2.67 (t, J = 7.4 Hz, 2H, -SCH₂-), 2.50 (td, J = 9.7, 4.4 Hz, 1H, -COCHCHCH₂-), 2.38 (t, J = 13.2 Hz, 1H, -COCH_aCH-), 2.31–2.22 (m, 1H), 2.16–2.09 (m, 3H), 2.11 (s, 3H, -SCH₃), 1.93–0.97 (m, 17H), 1.26 (s, 3H, -CH₃), 1.14 (s, 3H, -CH₃), 1.10 (s, 3H, -CH₃), 1.03 (s, 3H, -CH₃), 1.03 (s, 3H, -CH₃), 0.95 (s, 3H, -CH₃), 0.93 (s, 3H, -CH₃), 0.77 (s, 3H, -CH₃). ¹³C NMR (100 MHz, CD₃OD) δ 214.1, 170.3, 88.8, 86.6, 85.0, 72.0, 58.4, 57.3, 56.9, 55.8, 53.0, 44.3, 41.7, 40.6, 39.2, 39.1, 38.7, 37.0, 35.3, 33.0, 30.9, 30.2, 28.6, 27.4, 26.9, 26.2, 25.9, 25.6, 24.4, 19.3, 17.1 (2C), 16.5, 16.1, 14.9. HRMS (ESI) *m/z* calcd C₃₅H₆₀NO₅S⁺ [M + H]⁺ 606.4187, found 606.4164.

Compound **10b**, yield: 92%. [α]_D²⁵ + 24.4 (c 1.0, CHCl₃); ¹H NMR (400 MHz, CDCl₃) δ 4.58 (dd, J = 10.6, 3.2 Hz, 1H, -COOCH-), 3.81 (br, 1H), 3.71 (dd, J = 9.6, 5.5 Hz, 1H, -COCH-), 3.66 (d, J = 6.3 Hz, 1H, -OCOCH-), 3.60 (br, 1H), 2.96 (d, J = 9.3 Hz, 1H, -COCH-), 2.54 (td, J = 9.8, 3.8 Hz, 1H, -COCHCHCH₂-), 2.38–2.16 (m, 3H), 1.92–0.81 (m, 24H), 1.21 (s, 3H, -CH₃), 1.19 (s, 3H, -CH₃), 1.10 (s, 3H, -CH₃), 1.04 (s, 3H, -CH₃), 0.96 (s, 3H, -CH₃), 0.90 (s, 6H, -CH₃ × 2), 0.76 (s, 3H, -CH₃). ¹³C NMR (100 MHz, CDCl₃) δ 211.0, 167.7, 87.6, 85.3, 83.7, 70.4, 57.2, 57.2, 55.9, 55.8, 54.2, 43.0, 40.4, 38.2, 38.1, 38.1, 37.8, 37.5, 36.4, 34.2, 31.9, 28.1, 27.7, 26.7, 26.2, 24.9, 23.8, 18.2, 18.2, 17.3, 16.6 (2C), 16.0, 15.6. HRMS (ESI) *m/z* calcd C₃₅H₅₉NO₅Na⁺ [M + Na]⁺ 596.4285, found 596.4266.

Compound **10c**, yield: 93%. [α]_D²⁵ + 22.5 (c 1.0, CHCl₃); ¹H NMR (400 MHz, CDCl₃) δ 7.36–7.25 (m, 5H, Ar-H × 5), 4.47 (dd, J = 10.2, 3.8 Hz, 1H, -COOCH-), 4.21 (dd, J = 11.3, 5.5 Hz, 1H, -OCOCH-), 3.70 (dd, J = 9.3, 5.8 Hz, 1H, -COCH-), 3.31–3.23 (m, 2H), 2.95 (d, J = 9.3 Hz, 1H, -COCH-), 2.85–2.85 (m, 1H), 2.53 (td, J = 9.6, 4.0 Hz, 1H, -COCHCHCH₂-), 2.32–2.14 (m, 2H), 1.94–0.75 (m, 17H), 1.19 (s, 3H, -CH₃), 1.18 (s, 3H, -CH₃), 1.09 (s, 3H, -CH₃), 1.05 (s, 3H, -CH₃), 0.92 (s, 3H, -CH₃), 0.75 (s, 3H, -CH₃), 0.74 (s, 3H, -CH₃), 0.71 (s, 3H, -CH₃). ¹³C NMR (100 MHz, CDCl₃) δ 211.0, 168.9, 133.7, 129.3 (2C), 129.1 (2C), 127.9, 87.5, 85.3, 84.1, 70.4, 57.2, 55.9, 55.7, 54.3, 54.2, 43.0, 40.4, 39.6, 38.0, 37.7, 37.4, 36.5, 36.4, 34.2,

31.9, 27.8, 27.6, 26.9, 26.7, 26.2, 24.9, 23.8, 18.1, 16.6, 16.2, 16.0, 15.6. HRMS (ESI) m/z calcd $C_{39}H_{59}NO_5Na^+$ $[M + Na]^+$ 644.4285, found 644.4265.

Compound **10d**, yield: 81%. $[\alpha]_D^{22} + 32.8$ (c 0.40, CH_3OH); 1H NMR (400 MHz, CD_3OD) δ 7.37–7.26 (m, 5H, Ar-H \times 5), 4.69 (d, $J = 11.5$ Hz, 1H, $PhCH_a-$), 4.62 (dd, $J = 10.7, 4.9$ Hz, 1H, $-COOCH-$), 4.46 (d, $J = 11.5$ Hz, 1H, $PhCH_b-$), 4.29 (qd, $J = 6.5, 3.0$ Hz, 1H, $PhCH_2OCH-$), 4.13 (d, $J = 3.0$ Hz, 1H, $-OCOCH-$), 3.70 (dd, $J = 8.8, 6.6$ Hz, 1H, $-COCH-$), 3.06 (d, $J = 9.3$ Hz, 1H, $-COCH-$), 2.50 (td, $J = 9.6, 4.4$ Hz, 1H, $-COCHCHCH_2-$), 2.37 (t, $J = 13.2$ Hz, 1H, $-COCH_aCH-$), 2.13 (dd, $J = 12.9, 3.6$ Hz, 1H, $-COCH_bCH-$), 1.93–0.91 (m, 18H), 1.43 (d, $J = 6.6$ Hz, 3H, $-CHCH_3$), 1.25 (s, 3H, $-CH_3$), 1.14 (s, 3H, $-CH_3$), 1.10 (s, 3H, $-CH_3$), 1.03 (s, 3H, $-CH_3$), 1.01 (s, 3H, $-CH_3$), 0.93 (s, 3H, $-CH_3$), 0.82 (s, 3H, $-CH_3$), 0.76 (s, 3H, $-CH_3$). ^{13}C NMR (100 MHz, CD_3OD) δ 214.1, 168.8, 138.8, 129.4 (2C), 128.9, 128.8 (2C), 88.8, 86.6, 85.0, 74.0, 72.0, 72.0, 59.2, 58.4, 57.3, 56.9, 55.8, 44.3, 41.7, 40.6, 39.2, 39.0, 38.7, 37.0, 35.3, 33.0, 28.7, 27.4, 26.9, 26.2, 25.9, 25.6, 24.4, 19.3, 17.1, 17.0, 16.5, 16.4, 16.1. HRMS (ESI) m/z calcd $C_{41}H_{64}NO_6^+$ $[M + H]^+$ 666.4728, found 666.4702.

Compound **10e**, yield: 93%. $[\alpha]_D^{26} + 18.7$ (c 1.0, $CHCl_3$); 1H NMR (400 MHz, CD_3OD) δ 4.65 (dd, $J = 11.0, 5.5$ Hz, 1H, $-COOCH-$), 3.86 (d, $J = 17.3$ Hz, 1H, $-OCOCH_a-$), 3.80 (d, $J = 17.0$ Hz, 1H, $-OCOCH_b-$), 3.70 (dd, $J = 8.8, 6.6$ Hz, 1H, $-COCH-$), 3.07 (d, $J = 9.6$ Hz, 1H, $-COCH-$), 2.50 (td, $J = 9.8, 4.6$ Hz, 1H, $-COCHCHCH_2-$), 2.38 (t, $J = 13.3$ Hz, 1H, $-COCH_aCH-$), 2.13 (dd, $J = 13.1, 3.7$ Hz, 1H, $-COCH_bCH-$), 1.93–0.87 (m, 18H), 1.26 (s, 3H, $-CH_3$), 1.14 (s, 3H, $-CH_3$), 1.10 (s, 3H, $-CH_3$), 1.03 (s, 3H, $-CH_3$), 1.02 (s, 3H, $-CH_3$), 0.93 (s, 3H, $-CH_3$), 0.92 (s, 3H, $-CH_3$), 0.77 (s, 3H, $-CH_3$). ^{13}C NMR (100 MHz, CD_3OD) δ 214.1, 168.5, 88.9, 86.6, 84.5, 72.0, 58.5, 57.3, 57.0, 55.9, 44.3, 41.8, 41.1, 40.6, 39.3, 39.1, 38.7, 37.0, 35.3, 33.0, 28.4, 27.4, 26.9, 26.2, 25.9, 25.6, 24.5, 19.3, 17.1, 16.8, 16.6, 16.1. HRMS (ESI) m/z calcd $C_{32}H_{53}NO_5Na^+$ $[M + Na]^+$ 554.3816, found 554.3797.

Compound **10f**, yield: 90%. $[\alpha]_D^{30} + 21.9$ (c 1.0, $CHCl_3$); 1H NMR (400 MHz, CD_3OD) δ 4.63 (dd, $J = 10.7, 5.5$ Hz, 1H, $-COOCH-$), 4.28–4.25 (m, 1H, $-OCOCH-$), 3.70 (dd, $J = 8.7, 6.7$ Hz, 1H, $-COCH-$), 3.07 (d, $J = 9.6$ Hz, 1H, $-COCH-$), 3.02–2.89 (m, 2H), 2.50 (td, $J = 9.3, 4.5$ Hz, 1H, $-COCHCHCH_2-$), 2.37 (t, $J = 13.2$ Hz, 1H, $-COCH_aCH-$), 2.13 (dd, $J = 13.2, 3.6$ Hz, 1H, $-COCH_bCH-$), 1.93–0.87 (m, 18H), 1.28 (s, 3H, $-CH_3$), 1.14 (s, 3H, $-CH_3$), 1.10 (s, 3H, $-CH_3$), 1.03 (s, 3H, $-CH_3$), 1.02 (s, 3H, $-CH_3$), 0.93 (s, 3H, $-CH_3$), 0.90 (s, 3H, $-CH_3$), 0.77 (s, 3H, $-CH_3$). ^{13}C NMR (100 MHz, CD_3OD) δ 214.1, 169.5, 169.3, 88.8, 86.6, 84.8, 72.0, 58.4, 57.3, 57.0, 55.8, 51.1, 44.3, 41.7, 40.6, 39.2, 39.1, 38.7, 37.0, 35.3, 33.0, 31.7, 28.5, 27.4, 26.9, 26.2, 25.9, 25.6, 24.4, 19.3, 17.1, 16.9, 16.5, 16.1. HRMS (ESI) m/z calcd $C_{34}H_{55}NO_7Na^+$ $[M + Na]^+$ 612.3871, found 612.3847.

3.2. Cell Culture and NO Generation Assay

RAW264.7 cells were maintained in RPMI-1640 medium (containing 10% FBS) under a 5% CO_2 humidified condition at 37 °C and cellular NO release of treatment cells was evaluated using the Griess assay. Briefly, after pretreatment with the test compounds for 2 h, the experimental cells were treated with LPS (1 $\mu g/mL$) for another 24 h. Beyotime Griess reagent (China) was then used to assess NO levels in culture supernatants using a SpectraMax-M3 microplate reader (540 nm) as previously described [40].

3.3. Cell Viability

Cell survival rate was assessed in parallel with the NO generation assay using the MTT method as previously described [26]. Briefly, the compound-treated cells were further incubated with MTT reagent for 4 h. Subsequently, the resultant precipitates were dissolved in 150 μL DMSO and the OD was detected at 570 nm.

3.4. ELISAs

The experimental cells (0.5×10^4 per well) were cultured for 24 h, pretreated with 5c or HSS for 2 h and cotreated with 1 $\mu g/mL$ LPS for another 6 h (for TNF- α) or 24 h (for IL-1 β). The supernatant cytokine levels were next assessed using ELISA kits (Elabscience, Wuhan, China) based on the manufacturer's instructions [41].

3.5. Western Blotting

Target protein levels were estimated using Western blotting as published elsewhere [42,43]. Briefly, total cellular proteins of compound-treated cells were separated on the SDS-PAGE and blotted to the PVDF membrane (Millipore), then treated with Beyotime primary antibody (anti-iNOS (AF7281), anti-p- κ B (AF1870), anti- κ B (AF1282), anti-p-p65 (AN371), anti-p65 (AF1234), anti-p-ERK1/2 (AF1891), anti-ERK1/2 (AF1315), anti-p-SAPK/JNK (AF1762), anti-SAPK/JNK (AJ518), et al.) and Beyotime HRP-conjugated secondary antibody. The proteins were analyzed using chemiluminescence with the Beyotime ECL reagent.

3.6. Cellular Thermal Shift Assay (CETSA)

Protein–compound interactions in physiological environments were analyzed using CETSA [38,39]. RAW264.7 cells (2×10^7 cells/mL) were seeded for 24 h. After 2 h treatment with 5c (20 μ M), HSS (20 μ M), or DMSO, the cells were split into eight equal groups. The groups were heated for 3 min at 40, 43, 46, 49, 52, 55, 58, and 61 °C, followed by incubation at RT for 3 min. The cells then underwent five freeze–thaw cycles by placing in liquid nitrogen for 15 s followed by heating in a heating block at 30 °C for 3 min and brief vortexing. The lysates were centrifuged (12,000 rpm, 10 min) and the GR concentrations measured using Western blotting used GAPDH as the control.

3.7. Statistical Analyses

The data are represented as the means \pm SD and, when compared using Student's *t*-test, *p* < 0.05 values were statistically significant. All experiments were repeated in triplicate.

4. Conclusions

Pyxinol, the key pharmacophore of the liver metabolites of ginsenosides [12–14], was selected as the core skeleton for drug development in several groups. The effects of the dehydrogenation of pyxinol at C-12 on its potency have been rarely studied. In this study, 24 amino acid residue-conjugated 12-dehydropyxinol derivatives were produced and their inhibiting effects on LPS-triggered NO production were assessed. Compared with Y13, which was identified to be the most potent derivative of pyxinol, half of the 12-dehydropyxinol derivatives exhibited comparable potencies and several of them even showed much higher potencies than Y13. These results indicate that dehydrogenation at C-12 largely promotes the anti-inflammatory activity of C-3-modified derivatives. The SAR study further alluded that modification of 12-dehydropyxinol at C-3 with an *N*-Boc-protected aromatic amino acid led to an obvious increase in its anti-inflammatory activity, with 24R being the most preferred. Derivative 5c was then identified as exhibiting the most potent activity and relatively low cytotoxicity. Further studies have indicated that 5c exerted robust GR-independent anti-inflammatory activity by inhibiting the activation of NF- κ B and MAPK to suppress IL-1 β , TNF- α , and iNOS upregulation. The selective interaction of 5c with JNK is the possible mechanism for inhibiting MAPK activation. These data highlight that 12-dehydropyxinol derivatives hold immense drug-development potential owing to their anti-inflammatory activity.

Supplementary Materials: The following supporting information can be downloaded at: <https://www.mdpi.com/article/10.3390/molecules28031307/s1>, ¹H NMR and ¹³C NMR spectra of compounds.

Author Contributions: Conceptualization, G.Y. and H.Y.; methodology, G.Y., Y.W., X.M. and Y.D.; validation, Y.W., X.M. and Y.D.; formal analysis, Y.W.; investigation, Y.W., X.M., S.L., L.Y., M.G., X.Y., Z.S. and Y.D.; resources, G.Y. and H.Y.; data curation, G.Y.; writing—original draft preparation, G.Y. and H.Y.; writing—review and editing, G.Y.; visualization, G.Y., Y.W., X.M. and H.Y.; supervision, G.Y. and H.Y.; project administration, G.Y.; funding acquisition, G.Y. All authors have read and agreed to the published version of the manuscript.

Funding: This research was funded by Natural Science Foundation of Shandong Province (NO. ZR2022MB043), Talent Induction Program for Youth Innovation Teams in Colleges and Universities of Shandong Province, China Scholarship Council (No. 202108370160), Taishan Scholar Project, Graduate

Innovation Foundation of Yantai University and Students' Innovation and Entrepreneurship training Project of Yantai University.

Institutional Review Board Statement: Not applicable.

Informed Consent Statement: Not applicable.

Data Availability Statement: Not applicable.

Acknowledgments: The authors are grateful to National Demonstration Center for Experimental Pharmacy Education (Yantai University) for the support.

Conflicts of Interest: The authors declare no conflict of interest.

Sample Availability: Samples of the compounds are available from the authors.

References

1. Kesika, P.; Suganthy, N.; Sivamaruthi, B.S.; Chaiyasut, C. Role of gut-brain axis, gut microbial composition, and probiotic intervention in Alzheimer's disease. *Life Sci.* **2021**, *264*, 118627. [[CrossRef](#)] [[PubMed](#)]
2. Grivennikov, S.I.; Greten, F.R.; Karin, M. Immunity, inflammation, and cancer. *Cell* **2010**, *140*, 883–899. [[CrossRef](#)] [[PubMed](#)]
3. Annane, D.; Renault, A.; Brun-Buisson, C.; Megarbane, B.; Quenot, J.P.; Siami, S.; Cariou, A.; Forceville, X.; Schwebel, C.; Martin, C.; et al. Hydrocortisone plus Fludrocortisone for Adults with Septic Shock. *N. Engl. J. Med.* **2018**, *378*, 809–818. [[CrossRef](#)]
4. Horby, P.; Lim, W.S.; Emberson, J.R.; Mafham, M.; Bell, J.L.; Linsell, L.; Staplin, N.; Brightling, C.; Ustianowski, A.; Elmahi, E.; et al. Dexamethasone in Hospitalized Patients with COVID-19. *N. Engl. J. Med.* **2021**, *384*, 693–704.
5. Hyun, S.H.; Bhilare, K.D.; In, G.; Park, C.K.; Kim, J.H. Effects of Panax ginseng and ginsenosides on oxidative stress and cardiovascular diseases: Pharmacological and therapeutic roles. *J. Ginseng Res.* **2022**, *46*, 33–38. [[CrossRef](#)] [[PubMed](#)]
6. Kim, J.H.; Yi, Y.S.; Kim, M.Y.; Cho, J.Y. Role of ginsenosides, the main active components of Panax ginseng, in inflammatory responses and diseases. *J. Ginseng Res.* **2017**, *41*, 435–443. [[CrossRef](#)]
7. Yao, W.; Guan, Y.F. Ginsenosides in cancer: A focus on the regulation of cell metabolism. *Biomed. Pharmacother.* **2022**, *156*, 113756. [[CrossRef](#)]
8. Shi, Z.K.; Chen, H.Y.; Zhou, X.; Yang, W.; Lin, Y. Pharmacological effects of natural medicine ginsenosides against Alzheimer's disease. *Front. Pharm.* **2022**, *13*, 352332. [[CrossRef](#)]
9. Wang, M.; Li, H.; Liu, W.; Cao, H.; Hu, X.; Gao, X.; Xu, F.; Li, Z.; Hua, H.; Li, D. Dammarane-type leads panaxadiol and protopanaxadiol for drug discovery: Biological activity and structural modification. *Eur. J. Med. Chem.* **2020**, *189*, 112087. [[CrossRef](#)]
10. Karra, A.G.; Konstantinou, M.; Tzortziou, M.; Tsialtas, I.; Kalousi, F.D.; Garagounis, C.; Hayes, J.M.; Psarra, A.G. Potential Dissociative Glucocorticoid Receptor Activity for Protopanaxadiol and Protopanaxatriol. *Int. J. Mol. Sci.* **2018**, *20*, 94. [[CrossRef](#)]
11. Yang, Y.; Lee, J.; Rhee, M.H.; Yu, T.; Baek, K.-S.; Sung, N.Y.; Kim, Y.; Yoon, K.; Kim, J.H.; Kwak, Y.-S.; et al. Molecular mechanism of protopanaxadiol saponin fraction-mediated anti-inflammatory actions. *J. Ginseng Res.* **2015**, *39*, 61–68. [[CrossRef](#)]
12. Li, L.; Chen, X.; Li, D.; Zhong, D. Identification of 20(S)-protopanaxadiol metabolites in human liver microsomes and human hepatocytes. *Drug Metab. Dispos.* **2011**, *39*, 472–483. [[CrossRef](#)] [[PubMed](#)]
13. Wang, W.; Wu, X.; Wang, L.; Meng, Q.; Liu, W. Stereoselective Property of 20 (S)-Protopanaxadiol Ocotillol Type Epimers Affects Its Absorption and Also the Inhibition of P-Glycoprotein. *PLoS ONE* **2014**, *9*, e98887. [[CrossRef](#)] [[PubMed](#)]
14. Wang, W.; Wang, L.; Wu, X.; Xu, L.; Meng, Q.; Liu, W. Stereoselective formation and metabolism of 20(s)-protopanaxadiol ocotillol type epimers in vivo and in vitro. *Chirality* **2015**, *27*, 170–176. [[CrossRef](#)] [[PubMed](#)]
15. Feng, R.Q.; Liu, J.; Wang, Z.H.; Zhang, J.W.; Cates, C.; Rousselle, T.; Meng, Q.G.; Li, J. The structure-activity relationship of ginsenosides on hypoxia-reoxygenation induced apoptosis of cardiomyocytes. *Biochem. Biophys. Res. Commun.* **2017**, *494*, 556–568. [[CrossRef](#)]
16. Yang, G.Q.; Yang, Y.T.; Yang, Q.; Li, Y.; Jiang, Y.T.; Fu, F.H.; Wang, H.B. Novel Fluorescent Pyxinol-Based Probes: Design, Synthesis and Biological Evaluation. *Chin. J. Org. Chem.* **2017**, *37*, 2109–2114. [[CrossRef](#)]
17. Liu, J.L.; Liu, Y.H.; Yu, H.; Zhang, Y.; Hsu, A.C.Y.; Zhang, M.M.; Gou, Y.W.; Sun, W.; Wang, F.; Li, P.Y.; et al. Design, synthesis and biological evaluation of novel pyxinol derivatives with anti-heart failure activity. *Biomed. Pharmacother.* **2021**, *133*, 111050. [[CrossRef](#)]
18. Cao, Y.C.; Wang, K.Y.; Xu, S.; Kong, L.T.; Bi, Y.; Li, X.P. Recent Advances in the Semisynthesis, Modifications and Biological Activities of Ocotillol-Type Triterpenoids. *Molecules* **2020**, *25*, 5562. [[CrossRef](#)]
19. Zhang, D.D.; Cao, Y.C.; Wang, K.Y.; Shi, Z.Y.; Wang, R.D.; Meng, Q.G.; Bi, Y. Design, Synthesis, and Antibacterial Evaluation of Novel Ocotillol Derivatives and Their Synergistic Effects with Conventional Antibiotics. *Molecules* **2021**, *26*, 5969. [[CrossRef](#)]
20. Zhou, Z.; Ma, C.; Zhang, H.; Bi, Y.; Chen, X.; Tian, H.; Xie, X.; Meng, Q.; Lewis, P.J.; Xu, J. Synthesis and biological evaluation of novel ocotillol-type triterpenoid derivatives as antibacterial agents. *Eur. J. Med. Chem.* **2013**, *68*, 444–453. [[CrossRef](#)]
21. Ren, Q.W.; Yang, G.Q.; Guo, M.Q.; Guo, J.W.; Li, Y.; Lu, J.; Yang, Q.; Tang, H.H.; Fang, X.J.; Sun, Y.X.; et al. Design, synthesis, and discovery of ocotillol-type amide derivatives as orally available modulators of P-glycoprotein-mediated multidrug resistance. *Eur. J. Med. Chem.* **2019**, *161*, 118–130. [[CrossRef](#)] [[PubMed](#)]
22. Zhang, Y.K.; Zhang, H.; Zhang, G.N.; Wang, Y.J.; Kathawala, R.J.; Si, R.; Patel, B.A.; Xu, J.; Chen, Z.S. Semi-synthetic ocotillol analogues as selective ABCB1-mediated drug resistance reversal agents. *Oncotarget* **2015**, *6*, 24277–24290. [[CrossRef](#)] [[PubMed](#)]

23. Wang, C.; Gao, M.; Liu, S.; Zou, Z.; Ren, R.; Zhang, C.; Xie, H.; Sun, J.; Qi, Y.; Qu, Q.; et al. Pyxinol bearing amino acid residues: Easily achievable and promising modulators of P-glycoprotein-mediated multidrug resistance. *Eur. J. Med. Chem.* **2021**, *216*, 113317. [[CrossRef](#)] [[PubMed](#)]
24. Wang, Y.J.; Zhang, D.D.; Ma, G.S.; Su, Z.Y.; Liu, M.M.; Wang, R.; Meng, Q.G.; Bi, Y.; Wang, H.B. Design, synthesis, and biological evaluation of ocotillol derivatives fused with 2-aminothiazole via A-ring as modulators of P-glycoprotein-mediated multidrug resistance. *Eur. J. Med. Chem.* **2022**, *243*, 114784. [[CrossRef](#)]
25. Zhang, Z.Y.; Zeng, X.M.; Zhang, S.Y.; Zhou, Y.Y.; Zhou, Z.W. Novel ocotillol-derived lactone derivatives: Design, synthesis, bioactive evaluation, SARs and preliminary antibacterial mechanism. *Mol. Divers.* **2022**, *26*, 2103–2120. [[CrossRef](#)]
26. Yang, G.; Gao, M.; Sun, Y.; Wang, C.; Fang, X.; Gao, H.; Diao, W.; Yu, H. Design, synthesis and anti-inflammatory activity of 3-amino acid derivatives of ocotillol-type saponinins. *Eur. J. Med. Chem.* **2020**, *202*, 112507. [[CrossRef](#)]
27. Sun, Y.; Fang, X.; Gao, M.; Wang, C.; Gao, H.; Bi, W.; Tang, H.; Cui, Y.; Zhang, L.; Fan, H.; et al. Synthesis and Structure–Activity Relationship of Pyxinol Derivatives as Novel Anti-Inflammatory Agents. *ACS Med. Chem. Lett.* **2020**, *11*, 457–463. [[CrossRef](#)]
28. Pan, C.H.; Shan, H.J.; Wu, T.Y.; Liu, W.; Lin, Y.W.; Xia, W.Y.; Wang, F.; Zhou, Z.B.; Yu, X.W. 20(S)-Protopanaxadiol Inhibits Titanium Particle-Induced Inflammatory Osteolysis and RANKL-Mediated Osteoclastogenesis via MAPK and NF-kappa B Signaling Pathways. *Front. Pharm.* **2019**, *9*, 1538. [[CrossRef](#)]
29. Yang, G.Q.; Li, Y.; Yang, Q.; Yue, X.; Yao, L.; Jiang, Y.T. Simple and Efficient Synthesis of Pseudoginsenoside HQ. *Chin. J. Org. Chem.* **2017**, *37*, 1530–1536. [[CrossRef](#)]
30. Cinelli, M.A.; Do, H.T.; Miley, G.P.; Silverman, R.B. Inducible nitric oxide synthase: Regulation, structure, and inhibition. *Med. Res. Rev.* **2020**, *40*, 158–189. [[CrossRef](#)]
31. Chen, X.T.; Meng, F.Y.; Zhang, J.T.; Zhang, Z.J.; Ye, X.; Zhang, W.K.; Tong, Y.Y.; Ji, X.R.; Xu, R.J.; Xu, X.L.; et al. Discovery of 2-((2-methylbenzyl)thio)-6-oxo-4-(3,4,5-trimethoxyphenyl)-1,6-dihydropyridine-5-carbonitrile as a novel and effective bromodomain and extra-terminal (BET) inhibitor for the treatment of sepsis. *Eur. J. Med. Chem.* **2022**, *238*, 114423. [[CrossRef](#)] [[PubMed](#)]
32. Mosser, D.M.; Edwards, J.P. Exploring the full spectrum of macrophage activation. *Nat. Rev. Immunol.* **2008**, *8*, 958–969. [[CrossRef](#)]
33. Pacher, P.; Beckman, J.S.; Liaudet, L. Nitric oxide and peroxynitrite in health and disease. *Physiol. Rev.* **2007**, *87*, 315–424. [[CrossRef](#)]
34. Lawrence, T. The nuclear factor NF-kappaB pathway in inflammation. *Cold Spring Harb. Perspect. Biol.* **2009**, *1*, a001651. [[CrossRef](#)]
35. Kaminska, B. MAPK signalling pathways as molecular targets for anti-inflammatory therapy—From molecular mechanisms to therapeutic benefits. *Biochim. Biophys. Acta-Proteins Proteom.* **2005**, *1754*, 253–262. [[CrossRef](#)] [[PubMed](#)]
36. Bi, W.Y.; Fu, B.D.; Shen, H.Q.; Wei, Q.; Zhang, C.; Song, Z.; Qin, Q.Q.; Li, H.P.; Lv, S.; Wu, S.C.; et al. Sulfated Derivative of 20(S)-Ginsenoside Rh2 Inhibits Inflammatory Cytokines Through MAPKs and NF-kappa B Pathways in LPS-Induced RAW264.7 Macrophages. *Inflammation* **2012**, *35*, 1659–1668. [[CrossRef](#)]
37. Shoaib, R.M.; Ahmad, K.A.; Wang, Y.X. Protopanaxadiol alleviates neuropathic pain by spinal microglial dynorphin A expression following glucocorticoid receptor activation. *Br. J. Pharmacol.* **2021**, *178*, 2976–2997. [[CrossRef](#)] [[PubMed](#)]
38. Kawatkar, A.; Scheffter, M.; Hermansson, N.O.; Snijder, A.; Dekker, N.; Brown, D.G.; Lundbäck, T.; Zhang, A.X.; Castaldi, M.P. CETSA beyond Soluble Targets: A Broad Application to Multipass Transmembrane Proteins. *ACS Chem. Biol.* **2019**, *14*, 1913–1920. [[CrossRef](#)] [[PubMed](#)]
39. Jafari, R.; Almqvist, H.; Axelsson, H.; Ignatushchenko, M.; Lundbäck, T.; Nordlund, P.; Martinez Molina, D. The cellular thermal shift assay for evaluating drug target interactions in cells. *Nat. Protoc.* **2014**, *9*, 2100–2122. [[CrossRef](#)]
40. Zhu, X.; Wang, X.; Ying, T.; Li, X.; Tang, Y.; Wang, Y.; Yu, T.; Sun, M.; Zhao, J.; Du, Y.; et al. Kaempferol alleviates the inflammatory response and stabilizes the pulmonary vascular endothelial barrier in LPS-induced sepsis through regulating the SphK1/S1P signaling pathway. *Chem. Biol. Interact.* **2022**, *368*, 110221. [[CrossRef](#)]
41. Zhao, J.; Ling, L.; Zhu, W.; Ying, T.; Yu, T.; Sun, M.; Zhu, X.; Du, Y.; Zhang, L. M1/M2 re-polarization of kaempferol biomimetic NPs in anti-inflammatory therapy of atherosclerosis. *J. Control. Release* **2023**, *353*, 1068–1083. [[CrossRef](#)] [[PubMed](#)]
42. Yang, Y.T.; Guan, D.K.; Lei, L.; Lu, J.; Liu, J.Q.; Yang, G.Q.; Yan, C.H.; Zhai, R.; Tian, J.W.; Bi, Y.; et al. H6, a novel hederagenin derivative, reverses multidrug resistance in vitro and in vivo. *Toxicol. Appl. Pharmacol.* **2018**, *341*, 98–105. [[CrossRef](#)] [[PubMed](#)]
43. Fan, H.Y.; Wang, X.K.; Li, X.; Ji, K.; Du, S.H.; Liu, Y.; Kong, L.L.; Xu, J.C.; Yang, G.Q.; Chen, D.Q.; et al. Curcumin, as a pleiotropic agent, improves doxorubicin-induced nephrotic syndrome in rats. *J. Ethnopharmacol.* **2020**, *250*, 112502. [[CrossRef](#)] [[PubMed](#)]

Disclaimer/Publisher’s Note: The statements, opinions and data contained in all publications are solely those of the individual author(s) and contributor(s) and not of MDPI and/or the editor(s). MDPI and/or the editor(s) disclaim responsibility for any injury to people or property resulting from any ideas, methods, instructions or products referred to in the content.